

The long and the short of it: modelling double neutron star and collapsar Galactic dynamics

Paul D. Kiel^{1*}, Jarrod R. Hurley¹ and Matthew Bailes¹

¹Centre for Astrophysics and Supercomputing, Swinburne University of Technology, Hawthorn, Victoria, 3122, Australia

13 November 2018

ABSTRACT

Understanding the nature of galactic populations of double compact binaries (where both stars are a neutron star or black hole) has been a topic of interest for many years, particularly the coalescence rate of these binaries. The only observed systems thus far are double neutron star systems containing one or more radio pulsars. However, theorists have postulated that short duration gamma-ray bursts may be evidence of coalescing double neutron star or neutron star-black hole binaries, while long duration gamma-ray bursts are possibly formed by tidally enhanced rapidly rotating massive stars that collapse to form black holes (collapsars). The work presented here examines populations of double compact binary systems and tidally enhanced collapsars. We make use of BINPOP and BINKIN, two components of a recently developed population synthesis package. Results focus on correlations of both binary and spatial evolutionary population characteristics. Pulsar and long duration gamma-ray burst observations are used in concert with our models to draw the conclusions that: double neutron star binaries can merge rapidly on timescales of a few million years (much less than that found for the observed double neutron star population), common envelope evolution within these models is a very important phase in double neutron star formation, and observations of long gamma-ray burst projected distances are more centrally concentrated than our simulated coalescing double neutron star and collapsar Galactic populations. Better agreement is found with dwarf galaxy models although the outcome is strongly linked to the assumed birth radial distribution. The birth rate of the double neutron star population in our models range from $4 - 160 \text{ Myr}^{-1}$ and the merger rate ranges from $3 - 150 \text{ Myr}^{-1}$. The upper and lower limits of the rates results from including electron capture supernova kicks to neutron stars and decreasing the common envelope efficiency respectively. Our double black hole merger rates suggest that black holes should receive an asymmetric kick at birth.

Key words: binaries: close – stars: evolution – stars: pulsar – stars: neutron – Galaxy: stellar content – Gamma-rays: bursts

1 INTRODUCTION

Pulsars, magnetic oblate spheroids of nuclear densities 20 – 30 kilometers in diameter, have been found rotating at speeds of up to almost one thousand times a second (Hessels et al. 2006; see also Galloway 2008) in some of the most exotic settings in the known Universe. For example, some pulsars are found within X-ray binaries (Liu, van Paradijs & van den Heuvel 2007) and others with compact object companions in close binaries (Hulse & Taylor 1975) thought to be emitting gravitational radiation (see Landau & Lifshitz 1951; Paczyński 1967; Clark & Eardley 1977). Recently, the

number of known binary pulsars has been rapidly increasing (Lorimer et al. 2006a; Galloway et al. 2008). There are now in excess of 100 Galactic disk binary pulsars. This includes rotation powered pulsars (radio pulsars: ATNF Pulsar Catalogue Manchester, Hobbs, Teoh & Hobbs 2005¹) and accretion powered pulsars (X-ray binary pulsars: Liu, van Paradijs & van den Heuvel 2007; Galloway 2008; Galloway et al. 2008). More than 20 of these are accreting from a range of stellar masses and companion types (Galloway 2008), 9 are thought to orbit another neutron star (van den Heuvel 2007; Stairs 2008), while others (> 70) dwell in detached

* E-mail: pkiel@astro.swin.edu.au (PDK)

¹ <http://www.atnf.csiro.au/research/pulsar/psrcat/>

systems with white dwarfs companions (ATNF Pulsar Catalogue, Manchester et al. 2005) and possibly main sequence (MS) companions (Champion et al. 2008). From observations of pulsars in such systems it is possible to constrain computational modelling of binary evolutionary phases that are general to many non-pulsar related systems including, but not limited to, tidal evolution, Roche-lobe overflow and common envelope (CE) evolution. It is the most rapidly rotating pulsars that best constrain uncertainties in the theory related to these processes. Such work has been attempted in Kiel et al. (2008) and Kiel & Hurley (2009: KH09), where models of the complete Galactic pulsar population have been made. However, we note that these models are yet to include selection effects which are critical when interpreting the results of pulsar surveys (Taylor & Manchester 1977; Osłowski et al. 2009).

Short gamma-ray bursts provide an alternative method to study the physics of compact stars. Here compact stars are considered to be the most compact of remnants: neutron stars (NSs) and black holes (BHs). We define a double compact binary (DCB) to be any combination of these compact objects within a binary system (without any limit on the orbital period) and close DCBs are those systems with orbital periods of less than a few days. The DCBs that merge within the assumed 10 Gyr age of the Galaxy (i.e. during our simulations) are defined as coalescing DCBs. It is postulated that gamma-ray emission is produced during the coalescence of these systems and that radiation of gravitational waves occurs during the preceding in-spiral phase (Clark & Eardley 1977). In particular it is thought that short gamma-ray bursts are produced by coalescing double neutron star systems (Paczynski 1986). Gamma-ray burst observations are very interesting in themselves, however, DCB systems offer other observational features of importance. Not only can many tests of general relativity be performed but they offer insights into a host of observable phenomena (e.g. Taylor, Fowler & McCulloch 1979; Lyne et al. 2004). The formation of close DCBs requires two stars of sufficient mass to interact gravitationally, triggering mechanisms to decrease the separation between them during their stellar lifetimes. What seems to be the most important binary evolutionary mechanism in forming close DCBs is the common-envelope phase (Paczynski 1976) where the evolution following the first supernova (SN) generally requires at least one such event. The modelling of the CE phase is associated with much uncertainty (see, for example, Dewi, Podsiadlowski & Sena 2006; Belczynski et al. 2007a) and will be discussed further in the following section. Interestingly, Voss & Tauris (2003) found that 1/3 of BH-NS DCB systems can be formed via the direct-SN mechanism (Kalogera 1998) and therefore a CE phase is not required in all cases. Adding further uncertainty to the mix Brown (1995) suggested that unless the initial mass ratio is very close to unity NSs spiraling-in within a CE should always accrete enough matter to collapse and form BHs.

This work examines population characteristics of DCBs, including predictions of double neutron star (NS-NS) distributions and correlations between orbital properties and location. The results are extended to detail both long and short gamma-ray bursts (GRBs) and their progenitors, modelling tidally enhanced collapsars and coalescing DCBs. In particular, projected distances from the host galaxy of model

GRBs are compared to observations. No detailed conclusions from direct comparison to observations are attempted, as in Belczynski, Bulik & Rudak (2002) who account for redshift and different galaxy masses. Nor do we consider the evolution of systems in globular clusters (see e.g. Ivanova et al. 2008; Sadowski et al. 2008). Section 2 briefly outlines the population synthesis tool used in this body of work. The results are spread over Sections 3, 4 and 5, which examine the bound DCB and NS-NS populations (even if they go on to eventually coalesce), coalescing DCB populations and GRB populations, respectively.

2 POPULATION SYNTHESIS MODELS

The following work utilizes theoretical studies into NS binary and stellar evolution (Kiel et al. 2008) and Galactic kinematics (KH09). The modelling of stellar and binary evolution is performed by BINPOP, a Monte-Carlo population synthesis scheme that incorporates the detailed binary stellar evolution (BSE) code, developed by Hurley, Tout & Pols (2002) and updated in Kiel et al. (2008). BSE facilitates modelling of the latest theoretical stellar and binary evolution prescriptions such as: tides, stellar composition, magnetic braking, gravitational radiation, mass accretion over a range of timescales and realistic angular momentum evolution of pulsar systems. All of which are important evolutionary features when modelling populations of DCBs.

An aspect of binary evolution crucial to the formation and characteristics of close DCBs is common-envelope evolution (Paczynski 1976; Webbink 1984; Iben & Livio 1993). The treatment of CE evolution within BINPOP/BSE has previously been described in detail (Hurley, Tout & Pols 2002; Kiel & Hurley 2006). However, considering the potential influence of this phase on the outcomes of close binary population synthesis we also give an overview here so as to assist the reader in the interpretation of our results, noting that a full investigation of how uncertainties involved in modeling this phase affect the properties of the DCB populations will be left to future work. A CE phase is assumed to be initiated if a giant star (with a sizeable convective envelope) fills its Roche-lobe and the ensuing mass-transfer is calculated to occur on a dynamical timescale. The envelope of the giant then rapidly expands and envelops both the companion star and the degenerate core of the giant, thus forming a CE. As suggested by Paczynski (1976), the companion star and giant core will then spiral towards each other while transferring orbital energy to the envelope via dynamical friction. The eventual outcome of this process is essentially determined by a race between the spiral-in and the removal of the envelope owing to the energy transfer: if the companion and the giant core come into contact first then a merger results, otherwise the result is a close binary composed of the former core (now a remnant star) and the companion. Although some detailed hydrodynamic models of this process have been attempted (Bodenheimer & Taam 1984; Taam & Sandquist 2000; Ricker & Taam 2008) the treatment within population synthesis codes remains simplistic as a detailed theory is lacking. In BINPOP/BSE modelling of the CE phase is summed up by the equation:

$$\frac{M(M - M_c)}{\lambda R} = \frac{\alpha_{CE} M_c m}{2} \left(\frac{1}{a_f} - \frac{1}{a_i} \right) \quad (1)$$

which describes the energy balance between the binding energy of the envelope and change in orbital energy. These are related by an efficiency parameter, α_{CE} , which encapsulates the uncertainty of the model within what is known as the α -formalism (Nelemans & Tout 2005). Also included in the calculation are the mass of the giant star, M , the mass of the giant core M_c , the mass of the companion, m , the gravitational constant, G , the structure constant of the giant, λ , the radius of the giant, R , and the initial and final orbital separation, a_i and a_f . As documented in Hurley, Tout & Pols (2002) and Kiel & Hurley (2006), this is roughly the equivalent of using $\alpha'_{\text{CE}} = 1$ in the alternative formulation given by Iben & Livio (1993: where we have taken the liberty of using α'_{CE} to distinguish between the two methods) and thus corresponds to efficient transfer of energy within the CE. Kiel & Hurley (2006) found that using $\alpha_{\text{CE}} = 3$ aided comparison of the relative NS-low-mass X-ray binary and BH-low-mass X-ray binary formation rates to observations. Previous use of $\alpha_{\text{CE}} = 1$ produced a dearth of BH-low-mass X-ray binaries compared to NS-low-mass X-ray binaries.

Within the α -formalism the greater the value of α_{CE} the more efficient the spiral in process is at driving away the envelope. Values greater than unity may suggest an energy source other than gravitational potential energy is also important in driving off the envelope. The effect of the assumed value of α_{CE} (or α'_{CE}) on the results of binary population synthesis have been documented previously (e.g. Tutukov & Yungelson 1996; Belczynski, Bulik & Rudak 2002; Hurley, Tout & Pols 2002; Voss & Tauris 2003; Kiel & Hurley 2006). A large α_{CE} prescription is also equivalent to a large value of λ – a diffuse stellar envelope. In the past there have been three methods of accounting for the structure of the giant donor star with λ (see Voss & Tauris 2003 for a similar discussion on this point). One method is to include it with the CE efficiency and to simply vary a combined $\alpha_{\text{CE}}\lambda$ parameter (e.g. Belczynski et al. 2002a,b; Nelemans & Tout 2005; Pfahl, Podsiadlowski & Rappaport 2005; Belczynski et al. 2007a). Another method is to assume a constant value of λ (with 0.5 typically used) separate to the assumed α_{CE} value (numerically consistent with the previous method: Portegies Zwart & Yungelson 1998; Hurley, Tout & Pols 2002; Dewi, Podsiadlowski & Sena 2006; Kiel & Hurley 2006). The final method is to include an algorithm which provides varying values of λ depending upon (see Tauris & Dewi 2001) the mass (core and envelope) and stellar evolutionary phase of the donor star (e.g. Voss & Tauris 2003; Podsiadlowski, Rappaport, Han 2003; Kiel & Hurley 2006). Tauris & Dewi (2001) show that λ values may range between 0.02–0.7 (the average for massive stars being $\lambda = 0.1$: Dewi & Tauris 2001; Dewi, Podsiadlowski & Sena 2006). In this body of work we use a variable λ that ranges from 0.01–0.5 depending upon the donor type and we assume α_{CE} to be either 1 or 3.

Another feature of the CE phase which has been shown to clearly affect the resultant populations of double compact binaries is the possibility that CE initiated by stars on the Hertzsprung Gap (HG) always leads to coalescence (Belczynski et al. 2007a). Following this assumption Belczynski et al. (2007a) found that the merger rate of BH-BH binaries decreased by ~ 2 orders of magnitude compared to models without such a restriction. This concept is based on the study of Ivanova & Taam (2003) who, in agreement with

the suggestion of Podsiadlowski, Rappaport & Han (2003) found that all their detailed models in which a HG star initiates CE resulted in coalescence of the two cores. At this stage we do not impose such an outcome explicitly. However, the possibility of coalescence is increased by the use of a varying λ during CE. Here the value of λ may drop to as low as ~ 0.01 during the HG phase (e.g. Podsiadlowski, Rappaport & Han 2003) accounting for the lack of a convective envelope especially for those stars near the Hayashi track.

During the rapid and explosive formation of compact objects impulsive asymmetric mass-loss can lead to the transmission of momentum to the central compact object. To model this transfer of momentum we assume an instantaneous SN velocity kick for NSs in the form of a Maxwellian distribution with a dispersion of 190 km s^{-1} (see Kiel et al. 2008). For BH systems there are difficulties in statistically determining a realistic description for the SN kick magnitudes of the population. The magnitude of stellar BH velocity kicks is believed to vary between 0 and $\sim 300 \text{ km s}^{-1}$ (e.g. Jonker & Nelemans 2004; Willems et al. 2005). To account for this uncertainty we produce models where BHs receive no kicks or where BH kicks are drawn from a Maxwellian distribution with a dispersion of 190 km s^{-1} . We also can include electron capture SN (EC SN; Miyaji et al. 1980) events in our models. The capture of electrons onto primarily magnesium atoms within an oxygen-neon-magnesium core depletes the core of electron pressure resulting in the collapse and supernova explosion. The details of our EC SN model are found in Kiel et al. (2008) and here we provide models with and without this assumption. During EC SNe the SN kick is taken from a Maxwellian distribution with a dispersion assumed to be 20 km s^{-1} (typical values range anywhere from 0 – 50 km s^{-1}). The lower dispersion value arises because of the lower energy yield of EC SNe as compared to typical SNe.

Modelling of stellar and binary kinematic evolution within a galaxy is completed using BINKIN. This code, developed in KH09, solves four coupled equations of motion to evolve forward in time the galactic positions of systems of interest. BINKIN uses a recipe for the galactic gravitational potential structure, initial birth positions, initial system velocities and output from BINPOP to calculate the kinematic details for a population of stellar systems within a galaxy. The particular output from BINPOP of interest for BINKIN is information on SN recoil velocities (time, direction and magnitude) and the birth time of each system within the Galaxy (randomly selected from a flat distribution between 0 – 10 Gyr). Previously, both BINPOP (Kiel et al. 2008) and BINKIN (KH09) were used to examine pulsar systems exclusively. DCB and GRB systems, on the other hand, have not been considered directly or in such detail by us until now. We outline the modelling of GRBs systems below and consider their population characteristics in Section 5.

Gamma-ray bursts are found to occur on two timescales. There are long GRBs (LGRBs), where the observed bursting event occurs over timescales of typically 20s, and short GRBs (SGRBs), with a median burst duration of 0.3s (Woosley & Bloom 2006). The majority of population synthesis works have examined the evolution of what is believed to be SGRB progenitors – coalescing DCB systems (Portegies Zwart & Yungelson 1998; Bloom, Sigurdsson &

Pols 1999; Hurley, Tout & Pols 2002; Belczynski, Bulik & Rudak 2002; Voss & Tauris 2003; Belczynski et al. 2008; Sadowski et al. 2008) and similarly Paczyński (1990) modelled GRBs taking their locations as those of an old NS population. At present it is believed that LGRBs are formed during core-collapse type Ibc supernovae (SNe) of massive stars whose cores at the time of explosion are rapidly rotating (Woosley 1993; Woosley & Bloom 2006; termed as the ‘collapsar’ model by MacFadyen & Woosley 1999). Models suggest that the fall back accretion disks of SNe are more energetic and have longer timescales than models of double compact coalescence (Woosley 1993; Woosley & Bloom 2006). This leads to a longer GRB event for the former. Some alternative models of progenitor SGRBs are outlined in the review of Nakar (2007; and references within). These models include accretion induced collapse of NSs into BHs, type Ia SNe, magnetar giant flares and phase conversion from NSs to quark or hyper-stars.

Recently, realistic population synthesis models of GRBs have examined the formation and evolution of LGRBs produced from Population II progenitors (see Bogomazov, Lipunov & Tutukov 2008 and Detmers, Langer, Podsiadlowski & Izzard 2008) and Population III progenitors (Belczynski et al. 2007b). It has been shown that magnetic fields extract angular momentum from Wolf-Rayet (LGRB progenitor) cores, slowing the spin of the core below the rate required by GRB theory (Petrovic, Langer, Yoon & Heger 2005; Woosley 1993). Detailed modelling can produce rapidly rotating Wolf-Rayet cores at collapse if the initial stellar metallicity is reduced below solar quantities (Yoon, Langer & Norman 2006). However, in terms of population synthesis both Bogomazov, Lipunov & Tutukov (2008) and Detmers et al. (2008) assumed that the formation of LGRBs must have occurred within a binary system. Here a companion star can exert a tidal influence on the Wolf-Rayet core, keeping the system tidally locked until the SN and formation of LGRB and black hole. Bogomazov, Lipunov & Tutukov (2008) examined in some detail the effect modifying the metallicity and wind mass loss had on the formation of LGRBs, in line with the detailed models of Yoon, Langer & Norman (2006). Detmers et al. (2008) investigated, via detailed stellar models, whether the effect of tides in close binary systems at solar metallicities can spin up a Wolf-Rayet star sufficiently enough to form a collapsar-LGRB. Although Detmers et al. (2008) produced collapsar systems they found it could only arise from those systems that had some mass transfer and/or merger event during their lifetimes. Detmers et al. (2008) then perform a population synthesis study to compare their model birthrate to observations. They found that the tidally spun-up collapsar model could only produce a small fraction of the LGRB formation rate, however, carbon-oxygen and/or helium star mergers with BHs occur more readily and could possibly form some fraction of GRB systems.

For our LGRB models we follow the method of Detmers et al. (2008) which requires a system that contains a carbon-oxygen star to be tidally influenced by a BH. The rapidly rotating (tidally locked) carbon-oxygen star then goes on to form a BH and in the process a LGRB. It is not relevant if the resultant BH-BH system becomes disassociated. We consider a binary system to be tidally locked when the ra-

tio of carbon-oxygen star radius to the orbital separation is greater than 0.2 (Portegies Zwart & Verbunt 1996).

The focus of this paper is on DCB and GRB systems produced in population synthesis models. To compare with our previous pulsar population synthesis work we provide analysis of Model C''' from KH09. This model was introduced briefly in KH09 but is used in detail here. It involves the evolution of 10^9 binary systems which is two orders of magnitude greater than the main suite of models presented in KH09. Model C''' incorporates the favoured binary evolutionary model of Kiel et al. (2008), Model Fd, and the favoured kinematics of KH09. Details for the model can be found in Table 1 of Kiel et al. (2008) and Table 1 of KH09. For clarity we show the full set of possible parameters in BINPOP and BINKIN within Table 1 along with their values for Model C'''. To address some possible deficiencies of Model C''' we also examine the resultant DCB and GRB populations of an additional set of models that include different evolutionary assumptions. The model changes include assuming: (i) $\alpha_{CE} = 1$; (ii) BHs receive velocity kicks at birth (from the same SN kick distribution as NSs); and, (iii) BHs receive kicks *and* NSs may form via EC SN. Including these effects allow us to determine the extent by which such assumptions affect the final model DCB and LGRB populations. The initial number of binary systems in these additional models is 10^8 , an order of magnitude less than in Model C'''. As shown in KH09 this decrease in model initial binary number still provides statistical significant results for binary evolution and Galactic kinematics, while being preferable for computational efficiency. In our models we define the Galactic region of interest to include all stars with $R \leq 30$ kpc and $|z| \leq 10$ kpc. We note that when discussing DCB systems the order of compact star formation is depicted by the placement within the system name. For example the NS is created first in a NS-BH binary (i.e. before any SN the initially more massive star transfers much of its mass to the initially less massive star facilitating NS formation prior to BH formation).

3 BOUND DOUBLE NEUTRON STAR AND BLACK HOLE POPULATION CHARACTERISTICS

In this section, the population characteristics of DCBs are investigated. Model C''' was primarily used by KH09 to check the accuracy of scale heights drawn from models with smaller binary populations. The scale height is twice the e-folding distance of the population in $|z|$ and is calculated by counting all systems within 10 kpc of the plane. Exploring the DCB scale heights of Model C''', Table 2 shows the clear difference in NS-NS scale heights compared to those systems with at least one BH. This is primarily due to our assumption that BHs do not receive any velocity kick during their formation. It is interesting that BH-NS systems have a greater scale height than NS-BH systems. This results from the order in which the SN kick occurs, further discussion on this point follows below. For interest we note that very large distances from the plane can occur for DCB systems – up to 5.7 Mpc for the NS-NS systems – indicating that ejection of DCBs into the intergalactic medium can occur. Such systems are relatively rare, and are those which receive velocity

Table 1. Model C''' BINPOP and BINKIN parameters. See also Table 3 of Hurley, Tout & Pols (2002), Table 1 of Kiel & Hurley (2006), Kiel, Hurley, Murray & Hayasaki (2007), Table 1 of Kiel et al. (2008) and Table 1 of KH09. Note, the references within the table are: Kroupa, Tout & Gilmore (1993; KTG93), Belczynski, Kalogera & Bulik (2002; BKB02), Tauris & Manchester (1998; TM98), Yusifov & Kucuk (2004, YK04) and Paczyński (1990, Pac90). In this work we examine the effect changing some of these parameters have on the resultant population, in particular we include BH supernova kicks and electron capture SNe as well as decreasing the efficiency of the CE phase to $\alpha_{\text{CE}} = 1$.

BINPOP			
Parameter	Description	Value/ choice	Varied in Kiel et al. (2008)
Z	Zero-age main sequence metallicity	0.02	×
$M_{1i,\text{range}}$	Primary star birth mass range ($M_{1i,\text{min}} - M_{1i,\text{max}}$)	$5 - 80 M_{\odot}$	×
$\xi(M_1)$	Birth distribution of primary masses	KTG93	×
$M_{2i,\text{range}}$	Secondary star birth mass range ($M_{2i,\text{min}} - M_{2i,\text{max}}$)	$0.1 - 80 M_{\odot}$	×
$\phi(M_2)$	Birth distribution of secondary masses	$n(q) = 1$	×
$P_{\text{orbi},\text{range}}$	Orbital period birth range ($P_{\text{orbi},\text{min}} - P_{\text{orbi},\text{max}}$)	$1 - 3000$ days	×
$\Omega(\log P_{\text{orb}})$	Birth distribution of orbital period	Flat	×
e_i	Initial eccentricity distribution	0	×
α_{CE}	Common envelope efficiency parameter	3	×
λ	Binding energy factor for common envelope evolution	Variable (0.01 – 0.5)	×
$M_{\text{NS},\text{max}}$	Maximum NS mass	$3 M_{\odot}$	×
η	Reimers mass-loss coefficient	0.5	×
μ_{nHe}	Helium star wind mass loss efficiency parameter	0.5	×
B_{eml}	Binary (only) enhanced mass loss parameter	0.0	×
β_{wind}	Wind velocity factor	1/8	×
α_{wind}	Bondi-Hoyle wind accretion factor	3/2	×
Ξ_{wind}	Wind accretion efficiency factor	1.0	✓
ϵ_{nova}	Fraction of accreted matter retained in nova eruption	0.0001	×
E_{FAC}	Eddington limit factor for mass transfer	1.0	×
T_{flag}	Activates tidal circularisation	'on'	×
BH_{flag}	Allows velocity kick at BH formation	'off'	×
NS_{flag}	Takes NS/BH mass from BKB02	'on'	×
Be_{flag}	Allows Be star evolution and sets size of Be circumstellar disk	'off'	×
$\text{Be}_{\text{method}}$	Sets method used in Be/X-ray evolution: wind (< 0) or RLOF (> 0)	N/A	×
Be_{M}	Mass loss rate from Be star ($10^{-9} - 10^{-12} M_{\odot}/\text{yr}$)	N/A	×
τ_{B}	Pulsar magnetic field decay timescale	2 Gyr	✓
k	Pulsar magnetic field decay parameter during accretion	3000	✓
P_{flag}	Allows propeller evolution	'off'	✓
EC_{flag}	Triggers electron capture supernova evolution	'off'	✓
$f(P)$	Beaming fraction of pulsar according to TM98	'on'	✓
DL_{flag}	Allows pulsar death line	'on'	✓
SN_{link}	Initial pulsar parameters linked to supernova	'on'	✓
$P_{0\text{min}}^a$	Initial minimum pulsar spin period	0.02 s	✓
$P_{0\text{max}}$	Initial maximum pulsar spin period	0.16 s	✓
$B_{0\text{min}}$	Initial minimum pulsar magnetic field	5×10^{11} G	✓
$B_{0\text{max}}^b$	Initial maximum pulsar magnetic field	4×10^{12} G	✓
BINKIN			
Parameter	Description	Value/ choice	Varied in KH09
N	Number of systems evolved (also used in BINPOP)	10^9	✓
V_{σ}	Maxwellian dispersion for the supernova kick speed (also used in BINPOP)	190 km s^{-1}	✓
t_{max}	Age of the galaxy (also used in BINPOP)	10 Gyr	✓
Φ	Gravitational potential	Pac90	✓
α_{g}	Galaxy size and mass scaling parameter normalised to Milky Way	1	×
R_{init}	Galactic radial stellar birth distribution	YK04	✓
$ z_{\text{imax}} $	Maximum possible birth height off the galactic plane	0.075 kpc	✓
$ z_{\text{max}} $	Maximum height from the galactic plane used to calculate statistics	10 kpc	✓

^a For the SN link models, this value is the average initial spin period, $P_{0\text{av}}$, not the minimum

^b For the SN link models, this value is the average initial surface magnetic field, $B_{0\text{av}}$, not the maximum

Table 2. For each model the scale heights (kpc) and relative numbers are provided for all double compact binaries within 10 kpc of the Galactic plane at a Galactic age of 10 Gyr.

Model	System type	Scale height [kpc]	Relative number
C'''	NS-NS	1.53	0.003
	NS-BH	0.10	0.008
	BH-NS	0.24	0.006
	BH-BH	0.03	0.982
$\alpha_{\text{CE}} = 1$	NS-NS	0.90	0.002
	NS-BH	0.04	0.003
	BH-NS	0.15	0.008
	BH-BH	0.03	0.987
BH kicks	NS-NS	1.55	0.111
	NS-BH	1.18	0.063
	BH-NS	0.46	0.036
	BH-BH	0.78	0.790
BH kicks & EC SNe	NS-NS	0.73	0.290
	NS-BH	1.21	0.048
	BH-NS	0.37	0.048
	BH-BH	0.78	0.614

kicks greater than $\sim 500 \text{ km s}^{-1}$ (and integrated for close to 10 Gyr). Very few ($< 1\%$) BH-BH systems receive relatively large recoil velocities during SN solely from instantaneous mass loss (see Section 3.1). Model C''' produces a high relative number of BH-BH systems which remain bound after passing through two SNe as opposed to systems which receive one or two kicks in the process (see also the formation rates calculated in Section 4.1), once again a result of the assumption in Model C''' that BHs do not receive kicks.

When BHs are allowed to receive kicks the models show an expected increase in the scale height of BH-BH DCBs and all systems that include BHs. The relative number of BH-BH systems has also decreased, although they still dominate the DCB numbers. Such a large increase in scale heights of NS-BH systems, especially compared to BH-NS systems, is because BH kicks in our model are taken from a Maxwellian distribution with no regard to the amount of fall-back onto the BH. BHs with large mass progenitors ($M > 40 M_{\odot}$) have complete fall-back; therefore, binary systems are not unbound owing to instantaneous SN mass-loss from binary (as there is none) which allows the possibility of greater SN recoil velocities to be imparted onto the system than otherwise. Decreasing the efficiency of removing the envelope during the CE phase significantly reduces the NS-NS scale height. A lower α_{CE} results in more merger events during CE and tighter orbits of those systems that do survive. Although tighter pre-second supernova binary system would allow at first glance greater recoil velocities to occur (owing to larger allowed SN kicks) we find that the magnitude of the recoil velocity after the second SN in NS-NS systems is typically smaller ($\sim 200 \text{ km s}^{-1}$) than that in Model C''' ($\sim 500 \text{ km s}^{-1}$, see Figure 2), although the same range is covered. NS-NS systems in this model, therefore, typically merge on a smaller time scale than otherwise (see Section 4). As expected including EC SN kicks reduces the NS-NS scale height by half, while slightly decreasing the scale heights of other systems that include a NS. The relative number of NS-NS systems increases by two orders of magnitude in this model.

3.1 Recoil velocities

Figure 1 depicts the center of mass recoil velocities directly after the initial SN kick for Model C''' . These are shown as a function of final height from the Galactic plane for each system at the end of the simulation (or the point of coalescence). We compare recoil velocities of the four double compact binary types. We limit the figures to solely those of Model C''' , although our discussion of the resultant populations cover the other models. The initial SN velocity kick of those systems that form DCBs is typically less than the average velocity kick a NS in our models is given. This was also found by Voss & Tauris (2003, see Figure 11 of their paper) and arises because typical SN kick velocity magnitudes tend to disrupt binary systems, thus preventing DCB formation. NS-NS progenitors can survive the first SN with a greater recoil velocity than their NS-BH counterparts (who also receive a kick on the first SN). The cause of this is partly due to the greater average total system mass of NS-BH progenitors compared to that of NS-NS progenitors. However, for the formation of NS-BH binaries, the necessity of: mass transfer prior to any SN event, mass and orbital angular momentum loss via winds and the instantaneous mass loss during SN events (with the possibility of fall back onto the stellar remnants), greatly complicates matters. Other than a weak trend for NS-BH systems there does not seem to be any significant trend with final system height off the plane and the recoil velocity after the first SN.

Figure 2 illustrates the system centre-of-mass recoil velocity induced solely by the second SN. The range of resultant velocities is much greater than that provided by the first SN kick. Again, like Voss & Tauris (2003), we find that the double compact systems can survive, on average, greater second SN kicks than that which may occur for the first SN. Due to the massive nature of DCB progenitor stars it is typical that such systems have passed through at least one CE phase (see Sections 3.2 and 4; although see also Dewi, Podsiadlowski & Sena 2006). A large fraction of these systems have engaged in CE evolution in the intervening time between SN events because, when they survive the CE, the likelihood of binary disassociation owing to SNe decreases. Therefore, DCBs are typically tighter prior to the second SN compared to the first SN. Thus the SN kick must overcome greater orbital binding energy to disassociate the system which means a greater SN kick velocity is allowed that may in turn induce a greater recoil velocity into the system (ignoring mass loss). For some systems the only way that they may survive is from a sufficiently large and well directed kick, as discussed in Portegies Zwart & Yungelson (1998), and similar to the low-mass X-ray binary direct formation mechanism first recognised in Kalogera (1996). The mass of the double compact progenitors, at the second SN, is less than the mass at the first SN and as such the systems can end with much greater recoil velocities after the second SN.

We note that Figure 2 contains all systems that remain bound after the second SN regardless of whether they subsequently coalesce or not. Focusing on the NS-NSs (top left panel of Figure 2) we find that of the NS-NS systems in Model C''' that survived the two supernovae that 90% coalesce within 10 Gyr. Because of this the contours mainly trace the coalesced systems, which slope downwards in $|z|$ with increasing recoil velocity. This inverse trend arises be-

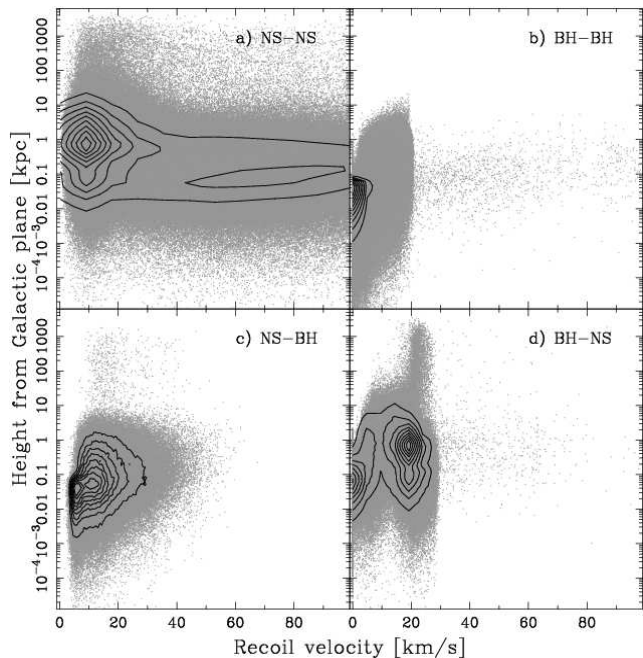


Figure 1. Distribution of the centre-of-mass recoil velocities after the 1st SN kick and the final system height above the plane in $|z|$ at 10 Gyr for all double compact systems that formed within Model C'''. This includes both coalesced and non-coalesced systems. Provided are contours ranging from 10% through to the outer contours of 90%. Clockwise from the top left is NS-NSs, BH-BHs, BH-NS (BH formed first) and NS-BH (NS formed first). Because of the large number of BH-BH systems (that may or may not coalesce) produced in this model we have had to limit the number of points we plot to every 10th (the contours are calculated from the complete sample).

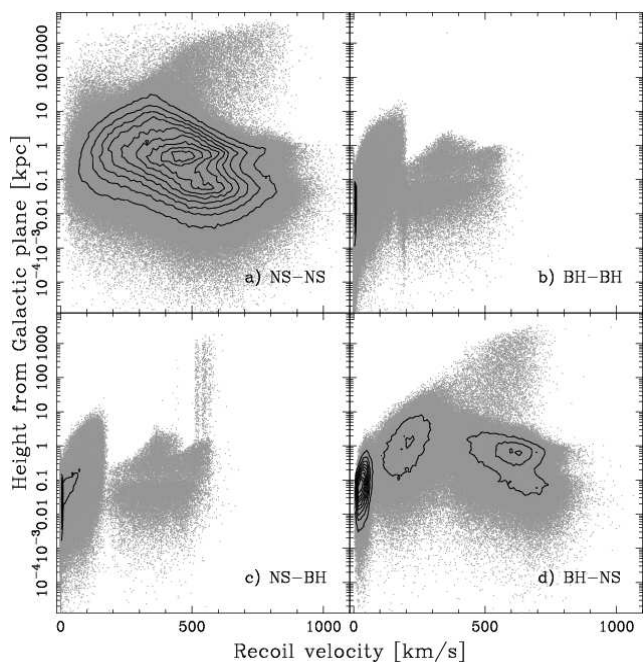


Figure 2. As for Figure 1 but now showing the centre-of-mass recoil velocity induced by the 2nd SN only. Contours are provided as in Figure 1.

cause we simply plot the merger site – the remnant evolution is ignored here – and systems that receive a greater recoil velocity (on average greater kick velocity and thus higher eccentricity) are more likely to merge faster than those that receive medium to low recoil velocities. However, the height off the plane for systems that remain bound and do not coalesce within our assumed age of the Galaxy is proportional to the recoil velocity of the second SN (and, of course, to the age of the system). This is shown by the population of points in the upper right of the panel (noting that the trend continues to low recoil velocity and $|z|$).

The top right panel depicts the BH-BHs. The majority of systems are contained at small recoil velocity values. However, there is a population of systems with recoil velocities greater than $\sim 200 \text{ km s}^{-1}$. These systems are ones that have coalesced within 10 Gyr of their formation. The NS-BH systems are given in the lower left panel of Figure 2. Both coalesced and bound NS-BH systems are tightly constrained to low recoil velocities and both tend to have increased $|z|$ values with higher recoil velocities, in this low recoil velocity range. However, beyond a recoil velocity of $\sim 200 \text{ km s}^{-1}$ there is a population of coalescing NS-BH systems which appear constrained to $|z| < 1 \text{ kpc}$ from the plane of the Galaxy. There is also a small population of NS-BH systems, which do not coalesce, that reside within a narrow recoil velocity band between 500 and 600 km s^{-1} . Such systems extend from $|z| \sim 0.01 \text{ kpc}$ up to $|z| \sim 1000 \text{ kpc}$. These systems do not receive SN velocity kicks for the second SN, so their formation and large $|z|$ does not rely on a sympathetic kick direction but instead on being tightly bound prior to BH formation and that for these systems there has been enough time in their evolution to reach such great distances.

The BH-NS systems within the bottom right panel contain two quite different distributions. The bound BH-NS systems extend from very low recoil velocities and small $|z|$ values to quite large recoil velocities and high $|z|$ values. In contrast the distribution of BH-NSs that coalesce begins at recoil velocities of $\sim 200 \text{ km s}^{-1}$ and $|z| \sim 1 \text{ kpc}$ and stretches to high recoil velocities and a height above the plane range of $0.0001 < |z| < 1 \text{ kpc}$. When BHs receive SN kicks their recoil velocity- $|z|$ distribution takes on the characteristics of the NS counterparts (although with generally smaller magnitudes). Providing NSs with the option to receive lower kick velocities during EC SNe assembles the resultant NS-NS distribution as an amalgamation between all the Model C''' distributions. When assuming a less efficient CE phase the NS-NS systems have a bimodal recoil velocity distribution with a group clustered between velocities of 0 km s^{-1} to $\sim 30 \text{ km s}^{-1}$ and another centered around $\sim 100 \text{ km s}^{-1}$ and extending either side by roughly 40 km s^{-1} .

3.2 Eccentricities and orbital periods

To examine NS-NS systems in greater detail Figure 3 depicts the eccentricity-orbital period population distribution that occurs at the simulation end. With greater numbers of NS-NSs now known (9 systems, 8 within the Galactic disk) and more realistic mass estimates of their stellar components available, recently it has become clear that this diagram sheds light on a possible inconsistency between observations and stellar binary theory (van den Heuvel 2007). Similar distributions to those shown in Figure 3 have been discussed

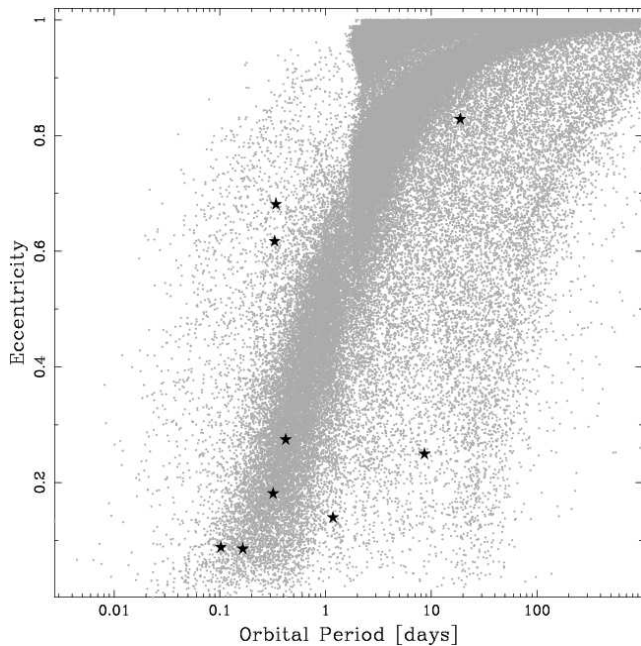


Figure 3. Eccentricity and orbital period parameter space snapshot of NS-NS systems at a Galactic age of 10 Gyr and within $4.5 < R < 12.5$ kpc. Included over our model points are 8 observed systems suspected to be NS-NSs according to van den Heuvel (2007) and Stairs (2008). The observed systems are, J0737-3039 (Lyne et al. 2004), J1518+4904 (Nice et al. 1996), B1534+12, J1811-1736, B1913+16 (Stairs 2004), J1756-2251 (Faulkner et al. 2005), J1829+2456 (Champion et al. 2004), J1906+0746 (Lorimer et al. 2006b) and B2127+11C (Anderson et al. 1990; detected within M15 with an eccentricity of 0.68 and orbital period of 8.05 hours).

in varying detail previously in population synthesis works (Portegies Zwart & Yungelson 1998; Bloom, Sigurdsson & Pols 1999; Voss & Tauris 2003; Ihm, Kalogera & Belczynski 2006). Unlike these previous works the systems considered here are restricted to reside within the solar neighbourhood ($4.5 \geq R \geq 12.5$ kpc). There is also no assumption on the ages of the observed NS-NS systems used for comparison – that is, the complete randomly born NS-NS model population is shown. Like Portegies Zwart & Yungelson (1998) this model finds that the addition of SN kicks within NS formation smears the eccentricity and orbital period distributions. Portegies Zwart & Yungelson (1998) also detail the importance of CE evolution in shaping the eccentricity-orbital period distribution. The typical formation pathway of NS-NSs systems that reside in Figure 3 pass through stable mass-transfer prior to any SN event. Owing to this mass-transfer either the mass ratio q inverts or, if $q \sim 1$, the secondary stars (initially less massive accreting stars) grow significantly more massive driving q to small values. After the first SN event the systems have a large range of eccentricities and orbital periods, however, with the onset of secondary star evolution these systems eventually pass through a CE evolutionary phase, circularising the orbit. The binary systems must survive CE and the secondary stars evolve to explode, forming NSs. It is the orbital parameters at the time of this SN and the event (kick) itself which is important in regulating the resultant eccentricity-orbital period NS-NS

population distribution. Such an evolutionary pathway compares well with the models of Portegies Zwart & Yungelson (1998), though, for young NS-NSs Portegies Zwart & Yungelson find many systems that pass through multiple CE phases between the two SN events. Multiple CE systems are also found in this model, however, these systems coalesce rapidly (few Myr), as such a discussion of these systems is left until Section 4.

The distribution of NS-NS systems within Figure 3 covers well the nine observed systems believed to be NS-NSs (van den Heuvel 2007; Stairs 2008). However, there is a greater relative number of observed NS-NSs with low eccentricities than that produced in this model. The majority of modelled systems within Figure 3 have eccentricities greater than 0.7 and only 17% have $e < 0.5$. Of the observed Galactic disk NS-NS systems 75% have $e < 0.5$. This discrepancy may be due to low number statistics owing to pulsar observational selection effects or incomplete theoretical modelling. One possible evolutionary phase that may assist in lowering the average eccentricity of model NS-NSs, as suggested by van den Heuvel (2007), is electron capture SNe (Miyaji et al. 1980; and as discussed in Section 2). EC SNe would induce smaller SN kicks into these systems potentially rendering them less eccentric. We are now in a position to examine this possibility with our EC SN model. We find that with EC SN included the percentage of systems with $e < 0.5$ increases only slightly to 20%. The overabundance of highly eccentric model NS-NS systems still remains a problem. We note here that a full parameter space search that includes EC SNe kicks can produce models that match the observed eccentricity distribution (Andrews, Kalogera & Belczynski, in preparation). However, we show here that this is not the case for standard model assumptions, of typical CE efficiencies and core collapse SN velocity kicks.

3.3 Eccentricities and height above the plane

It is also possible to examine the Galactic dynamics of double compact binaries to look for correlations between orbital properties and location. For such an analysis we make use of Figure 4 which depicts the $|z|$ -eccentricity parameter space for the four double compact binary types. The kinematics of NS-NS systems is as expected: the large relative number of eccentric systems typically extend in greater numbers further out in $|z|$ than less eccentric systems. The contour shows a strong trend within 1 kpc of increasing eccentricity with increasing $|z|$. However, there is effectively no variation above 1 kpc, the median eccentricity does not vary significantly with increasing height above the plane (see plus symbols within Figure 4). This is not the case for BH-BH systems of which the majority reside close to the Galactic plane with little to no eccentricity. Here the median eccentricity increases with rising $|z|$ until low number statistics dominate at $|z| \sim 2$ kpc. This suggests that the recoil velocity after the SN is greater with greater induced eccentricity. Because BH-BH systems receive no SN velocity kick, the resultant eccentricity and centre-of-mass recoil velocity relies upon the initial orbital stellar velocity components and the instantaneous mass loss from the system. According to the SN fall back prescription used within Kiel et al. (2008; from Belczynski, Kalogera & Bulik 2002) the greater the SN progenitor the less mass is lost from the system during SN and

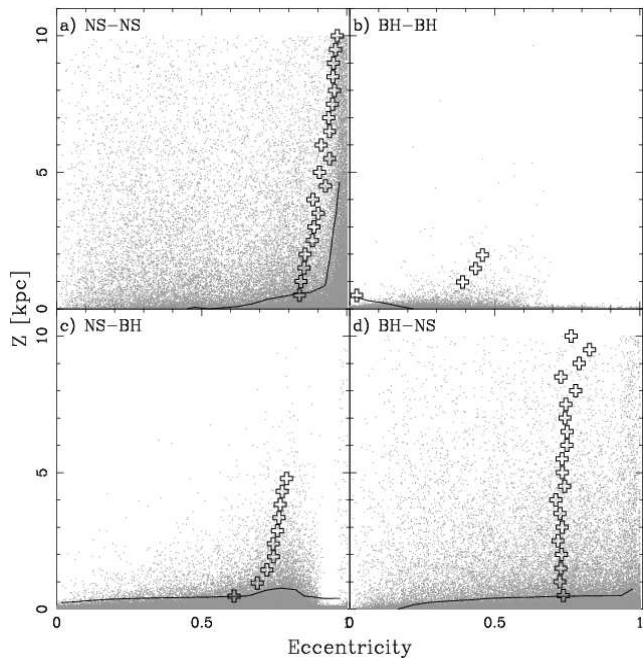


Figure 4. The eccentricity- $|z|$ distributions for each double compact system type. Top left is NS-NSs, top right BH-BHs, bottom left NS-BH where the NS formed first and bottom right BH-NS where the NS formed second. The 90% contour is shown for guidance. We also provide a representation of the median eccentricity of the distribution in steps of $|z| = 0.5$ kpc (plus symbols). When the statistical significance of each median eccentricity value is poor (less than 10 systems in the $|z|$ bin) we do not plot the point.

for many massive BHs complete fall back occurs. Therefore, in some instances there is little to no recoil velocity induced onto the system. Similar to BH-BH systems, although shifted to higher eccentricities, is the $|z|$ -eccentricity trend of NS-BH systems. There are more eccentric binaries in this population than in the BH-BH population. Owing to the kick velocity imparted during the NS formation, many systems are still eccentric when the BH is formed. The eccentricity ratio trend of the NS-BH systems, in $|z|$, is similar to that of the BH-BH population because the final SN produces a BH – the higher recoil velocity is directly proportional to the induced eccentricity. This is why there is no such trend in the BH-NS population: the eccentricity-recoil velocity link is weakened by the SN kick (the eccentricity depends mostly upon the kick strength, the recoil velocity upon the kick strength, direction and orbital parameters).

Because distributions such as in Figure 4 rely on SN kicks and binary evolution further observations of pulsar populations measuring parameters such as eccentricity, orbital period and height from the Galactic plane may help to constrain these evolutionary features. Of the 8 observed Galactic disk NS-NS systems all reside within $|z| < 1$ kpc and have a median eccentricity of 0.2. This is significantly less than the medium eccentricity produced in our model. Of the observed systems four reside within 0.05 kpc of the plane and while we do find that the median eccentricity of the model NS-NSs decreases with $|z|$ (for $|z| < 1$ kpc) we do not get below a value of 0.5. As shown in our analysis of Figure 3 this discrepancy is not resolved when accounting for

core collapse electron capture. Even limiting the region of the Galaxy considered to $|z| < 1$ kpc and $4.5 < R < 2.5$ kpc does not rectify the situation, only increasing the percentage of systems with $e < 0.5$ to $\sim 25\%$. Of course observational selection effects occur and unless these are also accounted for any direct observational comparisons are incomplete.²

3.4 Orbital period and Galactic kinematics

It is informative to examine the distribution of NS-NS systems in Galactic coordinates, in particular, to investigate the optimal regions within the Galaxy to survey when searching for such systems. Figure 5 depicts this for those NS-NSs with orbital periods less than 1 day in an Aitoff projection (as designed by Hammer 1892: see Steers 1970). We provide two populations: those with eccentricities less than 0.5 (grey circles) and those with eccentricities greater than 0.5 (dark circles). NS-NS systems, according to our model, will most likely be observed towards the Galactic centre. In Galactic Cartesian coordinates the distribution in R peaks at $R \sim 5$ kpc and the systems preferentially reside close to the Galactic plane. Unfortunately for observational predictions the populations with low and high eccentricities trace each other quite well. We provide the 9 detected NS-NS systems as a guide.

4 COALESCING DOUBLE COMPACT BINARIES

We now examine the population of double compact systems that coalesce within the simulations (i.e. within the assumed age of the Galaxy). The scale heights of these merger events are given in Table 3. The most interesting aspect of Table 3 is the scale height of coalescing NS-NSs compared to coalescing BH-NSs. It is surprising that the systems which typically receive greater combined recoil velocities (from both SN events) have a lower scale height. This scale height difference does not arise from low number statistics but rather from the shorter merger time scales of NS-NS systems compared to BH-NSs. Once a close NS-NS is formed, if it is to coalesce within a Hubble time, it will generally coalesce after a few Myr (see also Chaurasia & Bailes 2005). Whereas after BH-NS formation coalescence typically occurs after a few Gyr. Of course, this story changes somewhat when we include EC SN into the models. Now the scale height for merging double NSs increases owing to an increase in the typical merger time scale. Including kicks to BHs obviously helps to increase the scale height and decrease the merger time scale. Assuming $\alpha_{CE} = 1$ causes NS-NS systems to be closer after the final supernova explosion, which allows these systems to merge faster and decreases their merger scale height.

The coalescence times for the four system types in Model C''' are given in Figure 6 with each distribution normalised to unity. The coalescence times shown in Figures 6 to 8 are for those systems that merged during the simulation and represent the time each system took to coalesce

² Accounting for selection effects will be the focus of follow-up work (Kiel, Bailes & Hurley, in preparation)

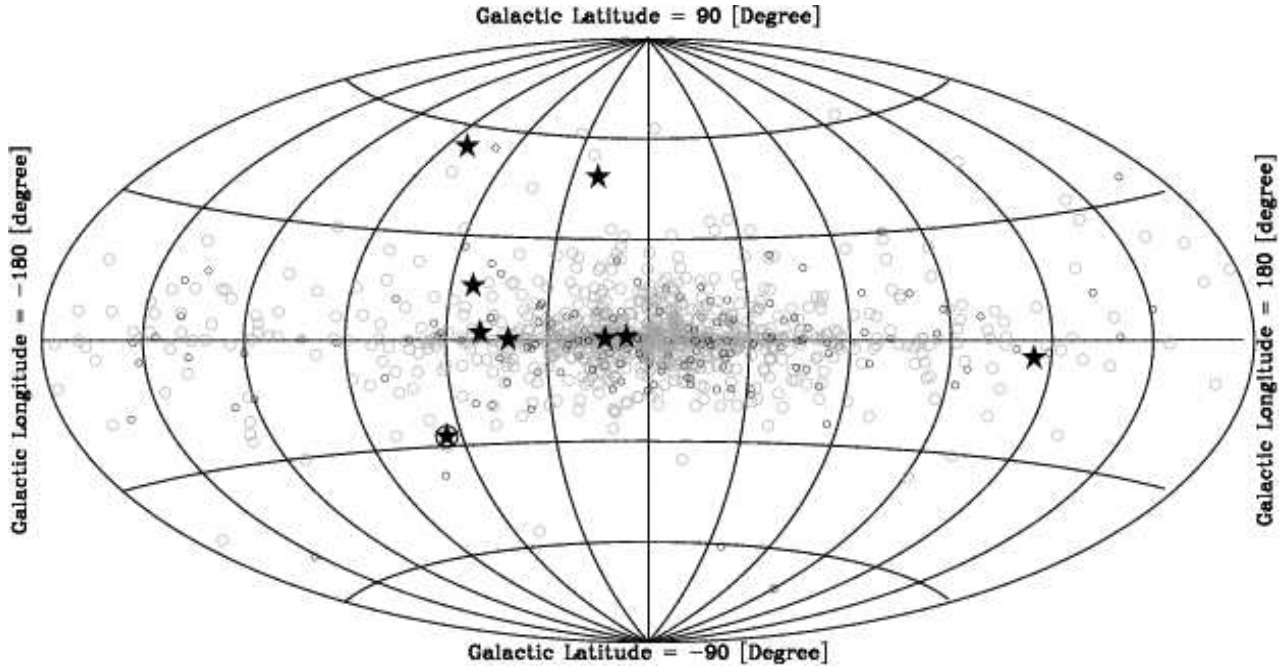


Figure 5. Aitoff projection of a subset of NS-NSs (circles) within $|z| < 5$ kpc of the Galactic plane and $R < 30$ kpc of the Galactic centre. The NS-NS systems shown all have $P_{\text{orb}} < 1$ day. Black circles represent systems with eccentricity greater than 0.5, the grey less than 0.5. Here a longitude of zero is the Galactic centre. For simplicity this figure has been made from Model C, that is, the number of underlying systems used to produce this plot is a factor of a 100 less than in Model C'''. We include the 9 detected NS-NS systems as black stars as found in the ATNF Pulsar Catalogue (the detected system enclosed in a large black circle is B2127+11C).

Table 3. Model scale heights (kpc) and relative numbers for all DCBs that have coalesced for the four models.

Model	System type	scale height [kpc]	Relative number
C'''	NS-NS	0.51	0.239
	NS-BH	0.11	0.029
	BH-NS	0.69	0.041
	BH-BH	0.05	0.691
$\alpha_{\text{CE}} = 1$	NS-NS	0.40	0.051
	NS-BH	0.06	0.001
	BH-NS	0.05	0.055
	BH-BH	0.05	0.893
BH kicks	NS-NS	0.53	0.536
	NS-BH	1.06	0.049
	BH-NS	0.69	0.029
	BH-BH	0.66	0.386
BH kicks & EC SNe	NS-NS	0.82	0.827
	NS-BH	1.07	0.018
	BH-NS	0.67	0.011
	BH-BH	0.65	0.144

(the length of time the DCBs lived). We note that there are in fact many more BH-BH and NS-NS systems than NS-BH and BH-NSs (an order of magnitude) and also we do not include the projected coalescence times for these systems that do not merge within our model. A model selection effect is then introduced at large times, where a turn over in the curves occur. Much can be gleaned from the incidence of the merger timescales peaks between each system type. The peaks of NS-NS and NS-BH systems correlate well, as do the peaks for BH-BH and BH-NSs. From this alone we see

the importance of the first SN on the final system merger timescale. The systems in which a NS forms from the first SN – imparting an asymmetric kick into the system – typically merge faster than those in which a BH is formed from the first SN. Also those systems that pass through multiple CEs merge fastest. In DCB formation mass transfer prior to any SN is an important factor in determining the number of CE events beyond the first SN event. If unstable mass transfer occurs prior to any SN and a CE occurs it is unlikely that two CE events will occur following the first SN event. However, if stable mass transfer occurs prior to the first SN it is possible that if the orbit is wide enough after the first SN then the companion star will initiate unstable mass transfer, while, say, core helium burning takes place, leaving a tight enough orbit for the resultant helium star to evolve and overflow its Roche-lobe and cause unstable mass transfer. Tightening the orbit once more. This is also more likely to occur – in a relative sense – for NS-NSs and NS-BHs than for BH-BHs and BH-NSs, because the NS SN kick can cause a tight binary system to expand more readily than for a BH SN event. These systems (NS-NSs and NS-BHs) also have a high eccentricity which allows unstable mass transfer to occur even though the separation of the two stars would otherwise be greater. The BH-BH and BH-NS systems that are wide (tens of thousands of solar radii) after the first SN must be wide to begin with. Unfortunately for these systems the relative stellar velocities are small which means that little to no eccentricities are imparted to the orbit. If after the first SN the secondary initiates mass transfer while core helium burning is taking place then, with such little eccentricities and large separations, these systems are likely to have stable mass transfer and expand their orbits. Even if

a CE phase does occur, after spiral in, the systems are still hundreds of solar radii apart.

The NS-NS and NS-BH systems that merge quickly all survive the first CE phase with a separation of $1 - 2 R_{\odot}$. The helium giant secondary star may then evolve to initiate another CE phase, in which the second NS is formed. Again the system survives with a separation of $1 - 2 R_{\odot}$. Such short orbital periods allows rapid (few Myr) coalescence. BH-BH and BH-NS systems that merge within 10 Gyr generally survive the CE phase with separations greater than $5 R_{\odot}$. The secondary star evolves and forms either a BH or NS but the separation at formation is typically of order $10 R_{\odot}$, for which a system will coalesce on a Gyr timescale. Therefore, these systems are susceptible to changes in the assumptions of CE evolution. However, usually such changes only result in shifts in the progenitor masses and orbital periods that produce such systems – the evolution pathway forming each system type remains viable (Kiel & Hurley 2006) but the relative numbers between system types change. Population birth/death rates (an important tool in model comparisons to observations) on the other hand are sensitive to changes in progenitor properties (Belczynski, Kalogera & Bulik 2002; O’Shaughnessy et al. 2005a). In particular rates are sensitive to changes in the initial stellar mass ranges and distributions and orbital period distributions (Kiel & Hurley 2006).

The asymmetric kicks in NS-NS and NS-BH systems also help in forming both very close and disrupted systems. This is indirectly shown by the greater width of the NS-NS merger time peak in Figure 6 to that of the NS-BH peak. The final NS-NS system separation depends upon the second SN kick, which is a random distribution, and causes a large array of separation values, which in turn forces variation into the coalescence times – smearing the merger time peak. The BH-BH merger time scale peak is not quite aligned to the BH-NS peak. Basically, this arises owing to the nature of gravitationally induced coalescence: heavier systems of the same separation after the second SN will naturally merger faster – even if the orbits are more circular. Of course, there is some cross over with system types and the mass transfer phases that occur which is why the four merger time curves have multiple peaks. However, the above analysis examines the *main* formation pathway for each system type.

We note here that this picture changes somewhat when the random birth age of each system is accounted for. In this case the number of merging systems steadily increases over time, reaching a maximum at the end of our simulation. Take NS-NS systems for example where the typical system age at the time of coalescence in Model C''' is $20 - 100$ Myr. Therefore, with random birth ages included the coalescence times for the model Galaxy begin at $\sim 10^7$ year. From that point on the continuous birth of systems between $0 - 10$ Gyr means that the number of coalescing systems increases until the end of star formation.

Of the NS-NS systems *observed* in the Galaxy approximately half are expected to merge within 10 Gyr – based on calculating the merger time scale owing to gravitational radiation from their orbital parameters. The double pulsar J0737-3039 has the shortest measured merger time scale of 85 Myr (Burgay et al. 2003). Therefore, the merger times of the observed NS-NSs all fall within the tail of our model distribution. This means that the model predicts that there is a large population of unobserved NS-NSs with merger time

Table 4. Formation rates for double compact binaries in a range of models over a span of 10 Gyr. Models considered are Model C''' from KH09 and three variations on this model which are, in turn, a reduction of α_{CE} , the inclusion of BH velocity kicks, and the inclusion of BH kicks as well as EC SNe.

Type	Model	C''' Myr ⁻¹	$\alpha_{\text{CE}} = 1$ Myr ⁻¹	BH kicks Myr ⁻¹	BH kicks + EC SNe Myr ⁻¹
NS-NS		38	4	37	162
NS-BH		10	2	4	5
BH-NS		10	7	3	3
BH-BH		820	750	42	45

scales shorter than those already observed. Future detection of such a system has the potential to significantly increase the empirical Galactic NS-NS merger rate (Kalogera et al. 2007).

When accounting for other evolutionary scenarios and assumptions the merger times of systems can change. Figures 7 and 8 depict the changes in merger times of NS-NS and BH-BH systems respectively, for a variety of models. When including EC SN evolution into our model the typical time NS-NS systems take to merge increases, as denoted by comparison of the peaks between the black line (Model C''') and the grey line (model including EC SN) within Figure 7. Such an outcome was expected because the small merger timescales of Model C''' are driven by strong well directed kicks that force the orbital separation to contract. Decreasing the common envelope efficiency from 3 to unity decreases the number of DCBs produced, which explains the erratic nature of the dashed curve within Figure 7. The $\alpha_{\text{CE}} = 1$ curve peaks at a slightly lower coalescence time than the other two models depicted. The less efficient the CE phase the greater the number of systems that merge or survive with smaller orbital separations. This last point means that systems which go on to form DCBs typically merge faster. There are, however, systems that normally would not have survived the second SN which now do (owing to the stronger gravitational well the exploding star resides in). There are a greater relative number of these large separation NS-NS systems in lower CE efficiency models, which can also be seen at long coalescence times in Figure 7. Note that the curves in Figures 6, 7 and 8 end prior to the age of the Galaxy because the number of systems drop to extremely low values. There are DCB populations with longer lifetimes than these end points suggest, however, the lifetimes are much too long to allow coalescence during our simulations (the DCB population characteristics are similar to the MSP-BH population described in detail within Section 4.4.2 of KH09). Figure 8 depicts BH-BH coalescence times for Model C''' (black line), BHs receiving kicks (grey line) and the $\alpha_{\text{CE}} = 1$ (dashed line) models. When SN kicks are introduced into BH evolution BH-BH systems merge slightly faster than otherwise. When $\alpha_{\text{CE}} = 1$ the coalescence time peaks at a similar value to that of Model C''' but there is a greater relative number of BH-BH systems that merge very quickly (< 0.1 Myr).

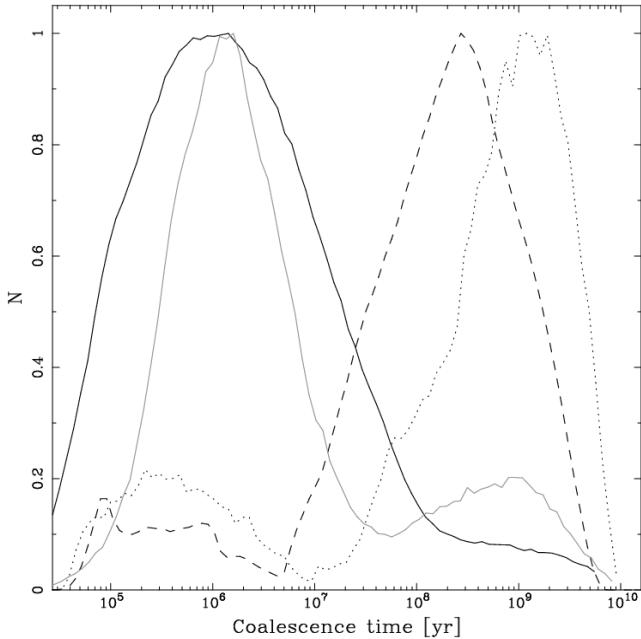


Figure 6. The coalescence times after DCB formation for Model C''' measured as the time elapsed between DCB formation and merger of the two stars. Full black line gives NS-NSs, dashed line is BH-BHs, full grey line is NS-BHs while the dotted line is BH-NSs. The distribution for each type of system is normalised to unity. This figure only counts those DCBs that coalesced within our simulation, which introduces a selection effect at large coalescence times.

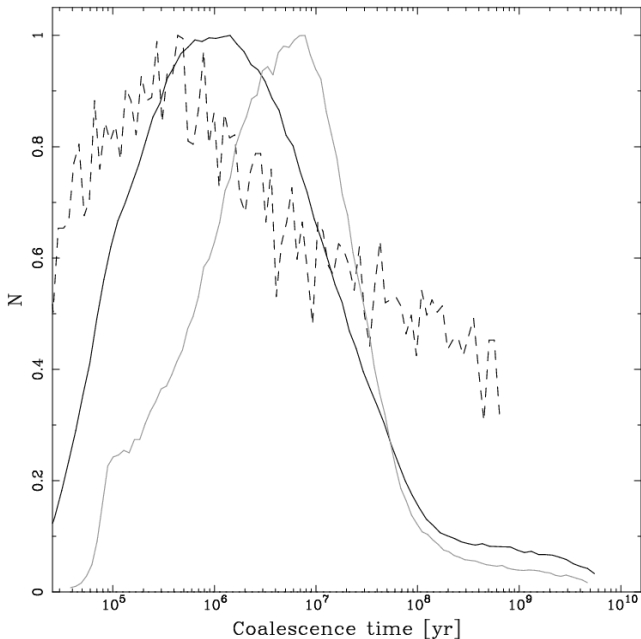


Figure 7. The coalescence times after NS-NS formation for variants on Model C''' . The full black line depicts Model C''' (as in Fig. 6). The model including electron capture SNe is given by the grey line and the dashed line depicts the model with $\alpha_{CE} = 1$. Each distribution is normalised to unity.

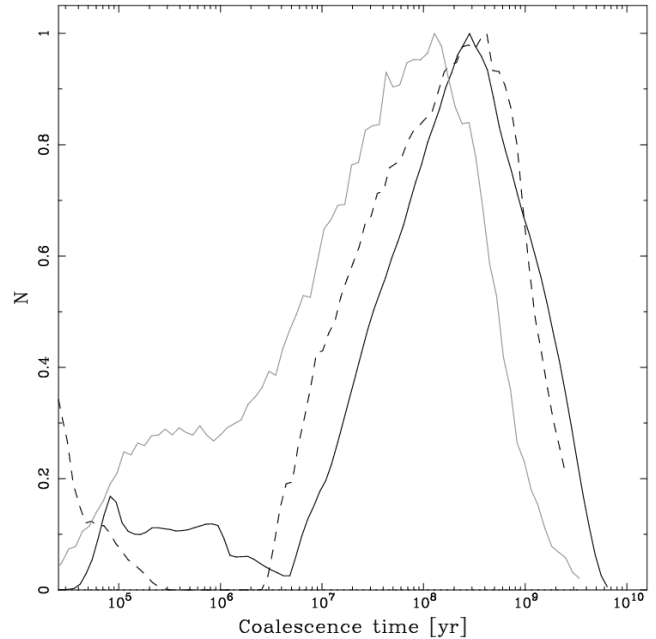


Figure 8. The coalescence times after BH-BH formation for variants on Model C''' . The full black line depicts Model C''' (corresponding to the dashed line in Fig. 6). The model including SN velocity kicks for BHs is denoted by the grey line and the dashed line depicts the model with $\alpha_{CE} = 1$. Each distribution is normalised to unity.

Table 5. As for Table 4 but now showing merger rates for DCBs.

Type	Model C''' Myr $^{-1}$	$\alpha_{CE} = 1$ Myr $^{-1}$	BH kicks Myr $^{-1}$	BH kicks + EC SNe Myr $^{-1}$
NS-NS	36	3	35	154
NS-BH	4	0.04	3	3
BH-NS	6	3	2	2
BH-BH	107	56	25	27

4.1 Formation and merger rates

In Tables 4 and 5 we show the formation and merger rates respectively for the four DCB system types in our models. To calculate the rates we first count the fraction of stars in the model that led to a Type II supernova, combine this with the assumption that the fraction of binaries in the Galaxy is 0.5, and normalize this to the empirical Galactic type II SNe rate ($\sim 0.01 \text{ yr}^{-1}$: Cappellaro, Evans & Turatto 1999). The relative numbers of the DCB systems and mergers are then calibrated against this to produce the rates. This method of calculation is commonly employed in binary population synthesis (Belczynski, Kalogera & Bulik 2002; Belczynski, Bulik & Rudak 2002; Voss & Tauris 2003; Pfahl et al. 2005, for example) so facilitates easy comparison with previous work. An alternative method uses the Galactic star formation rate (e.g. Kiel & Hurley 2006). With either method the uncertainties involved in the calibration make it more appropriate to discuss relative rather than absolute rates. This is also true of the uncertainties in rates owing to variations in the parameters of binary evolution models.

These uncertainties have been well documented in the past. For example, Belczynski, Bulik & Rudak (2002) find NS-NS merger rates in the range 3–300 Myr⁻¹ as a result of a comprehensive exploration of the available parameter space. While O’Shaughnessy et al. (2005b) favor models with NS-NS merger rates within the range 2.5–25 Myr⁻¹, although the total model range of merger rates extends far beyond these limits. Conversely, we find that rates quoted for a particular model (with a set choice of parameter values) vary by only a few percent at most with repeated realisations using distinct random number distributions (as was also found by Belczynski, Bulik & Rudak 2002). We note that in calculating our rates we have assumed an age of 10 Gyr for the Galaxy. If we instead take an age of 15 Gyr the quoted rates increase by less than 10%.

We quote rates for our Model C''' – with parameter values and distribution functions as listed in Table 1 – and a set of comparison models in which we alter the common-envelope efficiency parameter, the treatment of BH velocity kicks, and the possibility of NS formation via electron-capture SNe. A number of trends are immediately evident from Tables 4 and 5: (i) decreasing α_{CE} can reduce the rates by as much as an order of magnitude; (ii) without kicks for BHs the BH-BH rates are very high; and, (iii) the inclusion of EC SNe leads to a sharp increase in the NS-NS rates. Looking first at the NS-NS systems the merger rates of all models are in agreement with the empirical estimates of 3–190 Myr⁻¹ made recently by Kim, Kalogera & Lorimer (2006). They are also in agreement with the ranges found in the binary population synthesis works of Belczynski, Bulik & Rudak (2002) and O’Shaughnessy et al. (2005b), as is the noted behaviour of rates with variations in α_{CE} . The NS-NS merger rate found by Belczynski, Bulik & Rudak (2002) in their standard model was 53 Myr⁻¹ which is higher than in our Model C''' which has a rate of 36 Myr⁻¹. Belczynski, Bulik & Rudak (2002) used $\alpha'_{\text{CE}}\lambda = 1$ in their standard model which, assuming $\lambda = 0.5$, means $\alpha'_{\text{CE}} = 2$ and consequently a more efficient CE process than in Model C''' (which effectively uses $\alpha'_{\text{CE}}\lambda \simeq 1$: see Section 2). Thus the difference is consistent with the expected trend in CE efficiency but there are numerous more subtle differences between the models which could also play a role.

A noticeable outcome of our models is the high formation and merger rates for BH-BH binaries predicted by Model C''', which are above previous predictions in the literature (e.g. Lipunov et al 1997; Portegies Zwart & Yungleson 1998; Voss & Tauris 2003; Belczynski et al. 2007a), in some cases by more than an order of magnitude. Following the methodology of Belczynski et al. (2007a) the BH-BH merger rate of Model C''', given in Table 5, sets a detection rate for the current LIGO gravitational wave detector at approximately 1 yr⁻¹. LIGO has been running in detection mode for longer than this without a detection and therefore the Model C''' rate is inconsistent and thus an over-estimate. Reducing the efficiency of the CE spiral-in process halves the predicted BH-BH merger rate which is a step in the right direction. A further reduction result from the introduction of BH velocity kicks. In our model where BHs are given velocity kicks from the same distribution as for NSs (Maxwellian distribution with dispersion of 190 km s⁻¹) the BH-BH formation and merger rates decrease to 42 Myr⁻¹ and 25 Myr⁻¹, respec-

tively. We now find that the merger rate of NS-NS systems is larger than for BH-BH systems in agreement with the majority of previous works (other than Voss & Tauris 2003). This is further accentuated with the inclusion of EC SNe which increases the NS-NS merger rate to 154 Myr⁻¹ while leaving the BH-BH rate untouched. The models with BH velocity kicks lead to more plausible merger rate predictions as they are safely below the limit requiring a LIGO detection. They also agree well with the rates from the models of Belczynski, Kalogera & Bulik (2002) with similar input parameters and assumptions (see Belczynski et al. 2007a for a discussion of these rates).

As mentioned in Section 2, Belczynski et al. (2007a) describe a radically different evolutionary pathway to that presented in our models for Hertzsprung Gap stars which initiate CE. That is, these systems never survive CE. Belczynski et al. (2007a) show that adopting this pathway reduces the merger rates of BH-BH systems by a factor of 500 compared to a reduction of only a factor of 5 for NS-NS mergers. This swing would account for the stark difference in the BH-BH/NS-NS merger ratios found in our models compared to Belczynski et al. (2007a) and also makes a BH-BH gravitational wave detection less likely.

The detection of gravitational waves with Advanced LIGO (Lazzarini 2007) will go a long way towards constraining the NS-NS and BH-BH merger rates and importantly reduce the uncertainty in the BH-BH merger rates predicted by models. This has been highlighted previously by Belczynski et al. (2007a). The detection of a pulsar orbiting a black hole would also help to constrain many features of compact binary and pulsar evolution. This has been explored in Pfahl et al. (2005) and more recently in KH09 in terms of millisecond pulsar-black hole systems. Fortunately the models, owing to a greater number of possible observational comparisons, are more robust concerning predictions for coalescing NS-NS systems (as described above) and from this point on NS-NS systems are the focus of this work.

5 LONG AND SHORT GAMMA-RAY BURST GALACTIC KINEMATICS

We now examine the Galactic spatial distributions for our model GRBs, which require the following assumptions. We assume the coalesced NS-NSs which result in a BH are short gamma-ray bursts while our collapsar model (see Section 2) is assumed to form the long duration gamma-ray bursts. Figure 9 shows projected distances from the host galaxy center for our Model C''' coalescing DCB populations. The curves for all coalescing DCB system types are provided, noting that BH-BH mergers can not form gamma-ray bursts. We see that the different SGRB progenitor populations all follow very similar curves. The only slight difference is the BH-BH systems which receive reduced recoil velocities on average (see Figures 1 and 2) causing them to coalesce slightly closer to their original radial birth location compared to the other system types. Importantly, even the NS-NS cumulative curve follows the stellar radial birth cumulative curve (not shown) closely. At first glance such a result is surprising: previously it has been argued that because NSs receive large recoil velocities (Hobbs et al. 2005) SGRBs should not typically appear in star forming regions (Bloom, Kulkarni &

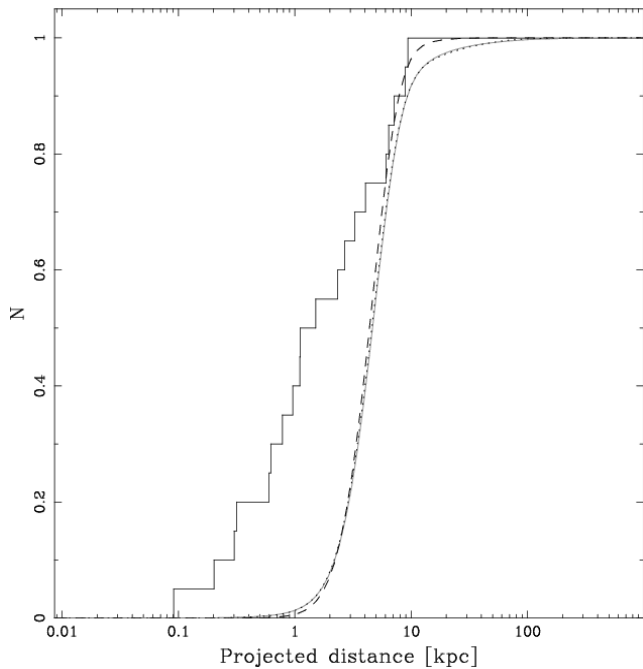


Figure 9. The projected distance from host galaxy for our different double compact systems that coalesce (SGRB progenitors). The projected distance is $\pi/4$ times the Model C''' Galactic radial distance (as in Voss & Tauris 2003). Full grey line gives NS-NSs, dashed line is BH-BHs and the dotted line is the two NS and BH combinations. We note that to model SGRBs via double compact coalescence requires that the progenitor system must contain at least one NS, for the formation of an accretion disk (see Voss & Tauris 2003 and references therein). The LGRB observations of Bloom, Kulkarni & Djorgovski (2002) are depicted by the jagged histogram.

Djorgovski 2002; Woosley & Bloom 2006). This is in contrast to LGRBs whose progenitors are thought to be massive stars – young stellar systems – which should correlate well with star forming regions (Bloom, Kulkarni & Djorgovski 2002). Yet owing to a population of close double compact systems, and thus a large population of systems that coalesce rather promptly (see Figure 6 which is in line with those produced in Belczynski, Bulik & Rudak 2002 and Voss & Tauris 2003), many of the model SGRBs merge at similar radial positions to their birth positions. As noted in Section 4 this feature of coalescing NS-NSs is also responsible for the smaller scale height of coalescing NS-NSs compared to that of BH-NS coalescence (see Table 3).

As shown in KH09 the form of the host galaxy potential plays an important role in determining the resultant stellar kinematics. The Galactic potential of our model, taken from Paczyński (1990), is more dominant than that used in Voss & Tauris (2003) but we do not see a significant difference in the SGRB distributions. We find that our model projected distances compare best with model f of Bloom, Sigurdsson & Pols (1998) which assumes a similar circular velocity (225 km s^{-1} compared to our 220 km s^{-1}) and an identical SN velocity kick dispersion of 190 km s^{-1} .

In Figure 9 we compare our SGRB models to observations of projected LGRB distances from their host galaxy centers according to Bloom, Kulkarni & Djorgovski (2002). We see that all Model C''' coalescing DCB populations fail

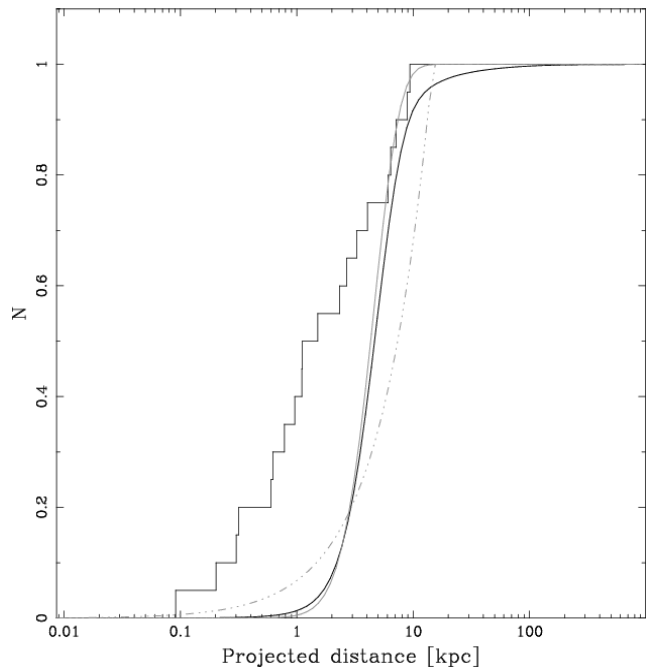


Figure 10. The projected distance from host galaxy for our different GRB progenitors. The projected distance is $\pi/4$ times the Model C''' GRB radial distances (as in Voss & Tauris 2003). Full black line gives NS-NS-SGRBs, full grey line is collapsar-LGRBs assuming the birth distribution of Yusufov & Kucuk (2004) and dashed-dotted grey line is the collapsar-LGRB distribution assuming a flat Galactic radial distribution between $0.01 < R < 20 \text{ kpc}$. The observations of Bloom, Kulkarni & Djorgovski (2002) are depicted by the jagged histogram.

to reproduce the LGRB observations. This is not exactly a surprise and agrees with previous studies (e.g. Bloom, Sigurdsson & Pols 1999; Belczynski, Bulik & Rudak 2002; Voss & Tauris 2003). What we emphasise here is that the difference does not arise from SNe recoil velocities but instead could be telling us something about the assumed initial birth distribution of the stars and binaries. In our model the birth distribution is based on observations, in particular the distributions of OB stars and HII in the Galaxy as determined by Yusufov & Kucuk (2004). Of course, at this stage, we are reliant upon making comparisons of two different populations, observed long gamma-ray bursts and model short gamma-ray bursts, and we note that statistics of observed SGRBs do not yet allow for meaningful comparisons (Savaglio, Glazebrook & Le Borgne 2009). Another factor is that our models so far have been for the Milky Way whereas the LGRB observations are predominantly from dwarf galaxies (see Figure 12 and associated text).

To understand the GRB distributions further we next provide results of LGRB models (rather than our previous SGRB models) to compare with the observations of *long*-GRBs (Bloom, Kulkarni & Djorgovski 2002). The method of determining LGRB progenitors is outlined in Section 2 and the important point to note is that the average age of each system (at the time of the LGRB) is young, less than $\sim 10 \text{ Myr}$, with little dependence of the formation mechanism on uncertain features of binary evolution. So it is safe to assume that the LGRBs will trace the birth positions

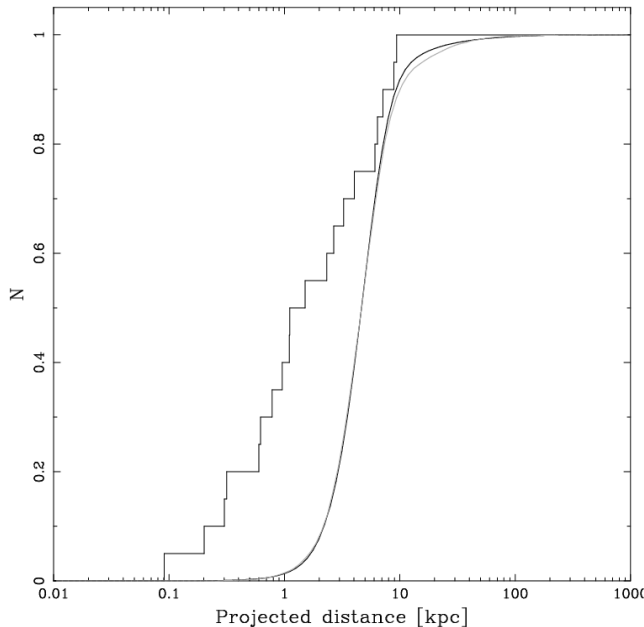


Figure 11. The projected distance from host galaxy for SGRBs of different models. The projected distance is $\pi/4$ times the Model C''' GRB radial distances (as in Voss & Tauris 2003). The grey line is the SGRB distribution assuming $\alpha_{\text{CE}} = 1$ and the full black line is Model C''' SGRBs. The observations of Bloom, Kulkarni & Djorgovski (2002) are depicted by the jagged histogram.

of their progenitors very closely. This is distinct from the SGRB models where the lifetimes of coalescing systems depend upon a number of evolutionary features and assumptions (common-envelope evolution and SNe velocity kicks, for example) as discussed in detail in Sections 3 and 4 and Belczynski, Bulik & Rudak (2002).

The model LGRB projected distance distribution is compared in Figure 10 to the LGRB observations and our previous NS-NS-SGRB distribution. This clearly shows that both our model GRBs – long and short – cannot reproduce the observations of GRB distances from their host galaxies. This is the case even when we allow an unrealistic radial birth description that is flat in Galactic radius (dashed-dotted line of Figure 10). Assuming a flat radial birth distribution does increase the number of LGRBs that occur in the inner Galactic regions compared to our standard LGRB and SGRB models (though not enough compared to observations), however, it also produces too many GRBs beyond $\sim 2 - 4$ kpc compared to the other models. Hence, the collapsar model requires birth placement which is incompatible with Population I stars in Milky Way like galaxies.

The majority of NS-NS systems merge rapidly when we assume $\alpha_{\text{CE}} = 1$, as shown in Figure 7. We compare this model SGRB projected distance distribution with LGRB observations and Model C''' in Figure 11. The EC SN model is not shown as it does not differ greatly from Model C''' and has typically longer merger times – which will not help here. The only noticeable difference between Model C''' and our $\alpha_{\text{CE}} = 1$ model is the distributions beyond about 10 kpc. Here the greater relative number of systems with large merger times cause the distribution to slope upward to unity slightly slower. Unfortunately it is the other end of

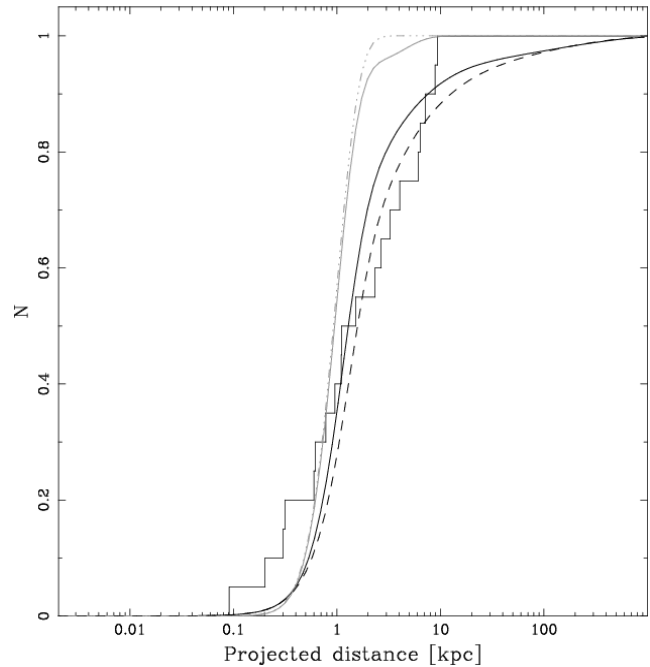


Figure 12. The projected distance from host dwarf galaxy for our different GRB progenitor systems. The projected distance is $\pi/4$ times the model radial distances (as in Voss & Tauris 2003). The dashed-dotted grey line is the collapsar-LGRB distribution assuming a scaled down model of our Galaxy ($\alpha_{\text{g}} = 0.01$). Full black line and the full grey line gives the NS-NS-SGRBs and collapsar-LGRBs within a scaled spherical potential ($\alpha_{\text{g}} = 0.1419$). The birth distribution for both dwarf galaxy models is that of Yuslifov & Kucuk (2004) scaled by $\alpha_{\text{g}} = 0.01$. The dashed line shows the NS-NS-SGRB distribution from a population of low metallicity stars ($Z = 0.0001$). The observations of Bloom, Kulkarni & Djorgovski (2002) are depicted by the jagged histogram.

the distribution, at small distances, where the models depart from observations.

This leads us to examine models of what is believed to be a more typical GRB host galaxy – a dwarf galaxy. Dwarf galaxies contain less mass than the Galaxy, with masses of order $10^9 M_{\odot}$, and are typically modelled by simple potentials such as in Bloom, Sigurdsson & Pols (1999). In fact, Belczynski, Bulik & Rudak found that the best match to GRB observations arose from a galaxy mass of $0.01 \times M_{\text{MW}}$ – the typical mass of a LGRB host galaxy. Bloom, Sigurdsson & Pols (1999) and Voss & Tauris (2003) also accounted for different galaxy masses, however, their initial stellar birth positions were not based on observations of OB stars but instead followed the exponential disk potentials – something which can be estimated from stellar kinematics (e.g. Kuijken & Gilmore 1989) and light profiles (e.g. de Vaucouleurs 1948). However, such observations measure stellar systems that differ from GRB progenitors.

To examine the effect such a small mass galaxy and gravitational potential has on our LGRB and SGRB populations we have produced two new galaxy models. The first model is a scaled down version of our Galaxy where, in line with Bloom, Sigurdsson & Pols (1999), Belczynski, Bulik & Rudak (2002) and Voss & Tauris (2003), we scale our previous model Galaxy mass, as described in KH09, by the scale

parameter α_g , giving us $M_{\text{galaxy}} = \alpha_g M_{\text{MW}}$. Assuming a constant density distribution between models,

$$\alpha_g M_{\text{MW}} \propto R_{\text{MW}}^3, \quad (2)$$

we then rescale the model scale lengths, scale heights and initial birth positions, also described in KH09, by $\alpha_g^{1/3}$. This first dwarf galaxy model assumes $\alpha_g = 0.01$ (giving us a similar galaxy mass and size of the favoured galaxy model in the work of Belczynski, Bulik & Rudak 2002), from which the mass of the dwarf galaxy is $M_{\text{galaxy}} = 1.419 \times 10^9 M_{\odot}$. The second model takes a spherical Hernquist (1990) potential as used in KH09 but scaled so the galaxy mass is the same as in our first dwarf galaxy model, thus $\alpha_g = 0.1419$. However, we keep $\alpha_g = 0.01$ when scaling the birth distribution in galactic z and R . We then evolve our SGRB and LGRB progenitor systems in each of the dwarf galaxy models. The resultant projected distance curves are compared with the observations of Bloom, Kulkarni & Djorgovski (2002) in Figure 12 (note we do not plot the SGRB model for the first scenario). All populations now more closely fit the observations than those in Figure 10, however, our LGRB models seem to over-estimate the number of GRB systems displaced between 1 – 10 kpc from the host galaxy central region and under-estimate the number of GRB systems displaced less than 1 kpc from the host galaxy. It is interesting that the best fit to the observations arises from our SGRB model, although this also under-estimates the number of GRB systems that occur in the inner galactic region.

The observed GRB host galaxies span a great range in red shift ($0 < z < 6.3$: Savaglio, Glazebrook & Le Borgne 2009) and as such many GRB host galaxies are low metallicity galaxies (Fruchter et al. 2006) – the average host galaxy metallicity being roughly one quarter solar (Savaglio, Glazebrook & Le Borgne 2009). The initial stellar metallicity has an important effect on governing the progenitor mass range for the formation of compact stars, in particular we note that NSs may emerge from lower mass stars in low metallicity environments than could possibly occur for higher metallicity populations. Therefore, compared to solar metallicity galaxies the resulting stellar and binary evolution in low metallicity galaxies could possibly extend the lifetimes of pre- and post-NS-NS formation, allowing such systems more time to evolve kinematically. This motivated us to examine what effect a low metallicity environment would have on the resultant SGRB population. To complete this we produced a SGRB model in our spherical Hernquist potential and assumed a metallicity of $Z = 0.0001$, which is depicted within Figure 12. Even with such a large difference in metallicity of the two SGRB models shown there does not appear to be a significant difference between their projected distance distributions. The number of model systems found close to the host galaxy (projected distance < 1 kpc) is still underestimated in this model although the slope of the distribution does become less steep. Although this suggests that metallicity does not play a major role in kinematics of SGRBs (and it does not within the assumptions used here), if mass loss rates are found to vary strongly with Z (Vink, de Koter & Lamens, 2001; Belczynski et al. 2010) and the kick strength prescription is allowed to vary with mass of the exploding star (e.g. from fallback as assumed in Belczynski et al. 2008) then there could indeed be a greater level of dependence on metallicity for SGRB kinematics.

Our models appear to confirm current observations that LGRBs are born in star forming regions (Kelly, Kirshner & Pahre, 2008; Dado & Dar 2009). We find that the final model GRB projected distance distributions are close to their respective birth distributions, while, when compared to observations, we under-estimate the number of GRBs that occur in the inner galactic region. Recently Fruchter et al. (2006) have suggested that there is a difference in LGRB and core collapse SN galactic environments. This could indicate that there is a difference in the birth distributions of the progenitors of these systems or that they arise from the same star formation distribution but from distinct progenitor mass ranges. Within our models we use the same birth distribution for both our LGRB and SGRB progenitors, namely the distribution according to Yusifov & Kucuk (2004) which should be realistic for SN progenitors and indeed was shown in KH09 to work well for pulsar models. However, as observations of the Galaxy suggest (Muno et al. 2006a; Muno et al. 2006b) there appears to be a relatively large population of massive stars within the inner ~ 300 pc. This may be the case for many galaxies and suggests that the Yusifov & Kucuk (2004) radial birth distribution is inappropriate for modelling the central galactic region. Thus it is quite possible that massive stellar systems may be born with a different galactic birth distribution than standard stars. In particular, the massive stellar birth distribution may be a combination of the the typical stellar distribution and a more centralised distribution. This scenario would suit both our models and observations that the material surrounding LGRBs is being highly irradiated by approximately 10 – 100 times more intensive UV radiation than that of the solar neighbourhood (Tumlinson et al. 2007) and that LGRBs occur in relatively low stellar density regions (Hammer et al. 2006; Tumlinson et al. 2007). It is also possible that this difference in the radial birth distribution may arise from open clusters with more massive stellar components falling quickly into the central galactic regions and becoming tidally disassociated (as in Muno et al. 2006b) or perhaps these more massive stars are formed from a metal poor distribution, allowing the birth of more massive stars that can evolve in isolation and still cause a LGRB (Yoon, Langer & Norman 2006).

The issue of whether or not LGRB and SGRB progenitors follow the same radial birth distributions has important consequences for the role that population synthesis studies can play in understanding GRB observations. If they do follow the same birth distribution then population synthesis models can not reliably distinguish between LGRB and SGRB progenitors via the resultant GRB-galaxy off-sets. This is because both GRB populations trace star forming regions (although given time SGRBs can also occur in old stellar systems). However, if the two GRB populations have different galactic birth distributions, as raised in the above discussions, then further modelling of GRB populations can figure prominently in shedding light on the continuing GRB progenitor problem.

6 SUMMARY

This work investigated the stellar, binary and Galactic kinematical evolutionary features of double compact binary systems and possible short gamma-ray burst (coalescing NS-

NSs) and long gamma-ray burst (tidally influenced collapsars) objects. The main conclusions from this investigation are summarised here:

- NS-NS systems are typically more kinematically active and have the greatest scale height of all DCBs, eclipsing the BH-BH population especially when BHs are assumed not to receive velocity kicks at birth. Including electron capture supernovae into models alters this somewhat. When assuming electron capture supernovae occur and that BHs receive kicks the BH-BH population has a comparable scale height to NS-NSs.

- We find the double neutron-star formation rate ranges between 4 Myr^{-1} and 162 Myr^{-1} . The lower value is set by assuming $\alpha_{\text{CE}} = 1$, the upper value by assuming EC SNe occurs. Our model without EC SNe and with $\alpha_{\text{CE}} = 3$ gives a double neutron-star formation rate of 38 Myr^{-1} .

- Our model double black-hole formation rate ranges between 42 Myr^{-1} and 820 Myr^{-1} . The lower value arises when we assume BHs receive kicks, the upper value arises when we do not assume BHs receive kicks.

- If NS-NSs merge it is likely they do so within a time scale of a few million years and with a merger rate that ranges between 3 Myr^{-1} and 154 Myr^{-1} for our models. The double neutron-star merger rates closely reflect their birth rates.

- BH-BH systems typically merge more slowly than NS-NS systems and this difference is enhanced when BHs do not receive kicks. The range of merger rates for double black holes is 25 Myr^{-1} to 107 Myr^{-1} . The most limiting factor is the addition of SN kicks to BH formation, while assuming $\alpha_{\text{CE}} = 1$ results in a merger rate of 56 Myr^{-1} . The maximum double BH merger rate arises when we assume they do not feel kicks at birth. Such a high merger rate suggest that at least one merger event should have been detected with LIGO. The null detection of gravitational waves by LIGO gives credence to the latest findings that BHs should receive kicks at birth.

- Common envelope evolution is reconfirmed to be a very important process for DCB formation. In particular, merger time scales are sensitive to the number of CE phases that occur within the intervening time between SN events. Decreasing the efficiency of the CE process decreases the typical merger time scale and final number of NS-NS systems. The CE phase is also important in shaping the final NS-NS eccentricity-orbital period distribution.

- We find good agreement of the shape of eccentricity-orbital period distribution when compared to observations but poor agreement with observations on the relative number of high eccentricity to low eccentricity systems. Including electron capture SN evolution into population synthesis models does not rectify the situation, as has been suggested previously.

- We find poor agreement between the projected distance of long gamma-ray bursts from their host galaxy and the projected distances of NS-NS systems within a Milky Way model.

- We find much better agreement between observations and models when the model galaxy mass and size is scaled down by a factor $\alpha_G = 0.01$. Owing to the short life times of our model systems (both short gamma-ray burst and long

gamma-ray burst) the final projected distances depend heavily on the assumed radial birth distribution.

ACKNOWLEDGEMENTS

PDK thanks Swinburne University of Technology for a PhD scholarship. The authors thank the referee for help with this paper.

REFERENCES

- Abramovici, A., et al. 1992, *Nature*, 256, 325
 Anderson S.B., Gorham P.W., Kulkarni S.R., Prince T.A., Wolszczan A., *Nature*, 1990, 346, 42
 Belczynski K., Bulik T., Rudak B., 2002, *ApJ*, 571, 394
 Belczynski K., Kalogera V., Bulik T., 2002, *ApJ*, 572, 407
 Belczynski K., Taam R.E., Kalogera V., Rasio F.A., Bulik T., 2007a, *ApJ*, 662, 504
 Belczynski K., Bulik T., Heger A., Fryer C., 2007b, *ApJ*, 664, 986
 Belczynski K., Kalogera V., Rasio, F.A., Taam R.E., Zezas A., Bulik T., Maccarone T.J., Ivanova N., 2008, *ApJS*, 174, 223
 Belczynski K., Tomasz B., Fryer C.L., Ruiter A., Valsecchi F., Vink J.S., Hurley J., 2010, accepted *ApJ*, astro-ph/0904.2784B
 Bloom J.S., Sigurdsson S., Pols O.R., *MNRAS*, 305, 763
 Bloom J.S., Kulkarni S.R., Djorgovski S.G., 2002, *ApJ*, 123, 1111
 Bodenheimer P., Taam R.E., 1984, *ApJ*, 280, 771
 Bogomazov A.I., Lipunov V.M., Tutukov A.V., 2008, *Astronomy Reports*, 53, 463
 Brown G.E., 1995, *ApJ*, 440, 270
 Burgay M., et al., 2003, *Nature*, 462, 531
 Cappellaro E., Evans R., Turatto M., 1999, *A&A*, 351, 459
 Champion D.J., Lorimer D.R., McLaughlin M.A., Cordes J.M., Taylor J.H., 2004, *MNRAS*, 350, L61
 Champion D.J., et al., 2008, *Science*, 320, 1309
 Chaurasia H.K., Bailes M., 2005, *ApJ*, 632, 1054
 Clark J.P.A., Eardley D.M., 1977, *ApJ*, 251, 311
 Dado S., Dar A., 2009, *ApJ*, 693, 311
 Detmers R.G., Langer N., Podsiadlowski Ph, Izzard R.G., 2008, *A&A*, 484, 831
 Dewi J. D. M., Tauris T. M., 2001, in Podsiadlowski P., Rappaport S., King A. R., D'Antona F., Burderi L., eds, ASP Conf. Ser. Vol. 229, *Evolution of Binary and Multiple Star Systems*. Astron. Soc. Pac., San Francisco, p. 255
 Dewi J. D. M., Podsiadlowski Ph., Sena A., 2006, *MNRAS*, 368, 1742
 de Vaucouleurs G., 1984, *AnAp*, 11, 247
 Fruchter A.S., et al., 2006, *Nature*, 441, 463
 Faulker A.J., et al. 2005, *ApJ*, 618, 119
 Galloway D.K., 2008, in Bassa C.G., Wang Z., Cumming A., Kaspi V.M., eds., AIP Conf. Ser. Vol. 938, *40 Years of Pulsars – Millisecond Pulsars, Magnetars, and More*, American Inst. of Physics, New York, p. 510
 Galloway D.K., Muno M.P., Hartman J.M., Psaltis D., Chakrabary D., 2008, *ApJS*, 179, 360
 Hammer E., 1892, *Petermanns Mitt.*, 38, 85

- Hammer F., Flores H., Schaere D., Dessauges-Zavadsky M., Le Floch E., Puech M., 2006, *A&A*, 454, 103
- Han Z., Podsiadlowski P., Eggleton P.P., 1995, *MNRAS*, 272, 800
- Hernquist L., 1990, *ApJ*, 356, 359
- Hobbs G., Lorimer D.R., Lyne A.G., Kramer M., 2005, *MNRAS*, 315, 543
- Hulse R.A., Taylor J.H., 1975, *ApJ*, 195, 51L
- Hurley J.R., Tout C.A., Pols O.R., 2002, *MNRAS*, 329, 897
- Iben I.Jr., Livio M., 1993, *PASP*, 105, 1373
- Ihm C.M., Kalogera V., Belczynski K., 2006, *ApJ*, 652, 540
- Ivanova N., Taam R.E., 2003, *ApJ*, 599, 516
- Ivanova N., Heinke C.O., Rasio F.A., Belczynski K., Fregeau J.M., 2008, *MNRAS*, 386, 553
- Jonker P.G., Nelemans G., 2004, *MNRAS*, 354, 355
- Kalogera V., 1996, *ApJ*, 471, 352
- Kalogera V., 1998, *ApJ*, 493, 368
- Kalogera V., Belczynski K., Kim C., O’Shaughnessy R., Willems B., 2007, *PhR.*, 442, 75
- Kiel P.D., Hurley J.R., 2006, *MNRAS*, 369, 1152
- Kiel P.D., Hurley J.R., Murray J.R., Hayasaki K., 2007, in Stefl S., Owocki S.P., Okazaki A.T., eds., *ASP Conf. Ser. Vol. 361, Active OB-Stars: Laboratories For Stellar and Circumstellar Physics*. ASP, San Francisco, p. 448
- Kiel P.D., Hurley J.R., Bailes M., Murray J.R., 2008, *MNRAS*, 388, 393
- Kiel P.D., Hurley J.R., 2009, *MNRAS*, 402, 1437 (KH09)
- Kim C., Kalogera V., Lorimer D.R., 2006, in Kapers L., van der Klis M., Wijers R., *New Ast. Rev.*, A Life with Stars. Elsevier, Amsterdam, in press, *astro-ph/0608280v1*
- Kelly P.L., Kirshner R.P., Pahre M., 2008, *ApJ*, 687, 1201
- Kroupa P., Tout C.A., Gilmore G., 1993, *MNRAS*, 262, 545
- Kuijken K., Gilmore G., 1989, *MNRAS*, 239, 571
- Landau L.D., Lifshitz E.M., 1951, *The classical Theory of Fields*, 1st English edn. Pergamon Press, Oxford
- Lazzarini A., 2007, Update from LIGO laboratory, LIGO Document G070649-00-M
- Liu Q.Z., van Paradijs J., van den Heuvel E.P.J., 2007, *A&A*, 469, 807
- Lorimer D.R., et al., 2006a, *MNRAS*, 372, 777
- Lorimer D.R., et al., 2006b, *ApJ*, 640, 428
- Lyne A.G., et al., 2004, *Science*, 303, 1153
- Manchester R.N., Hobbs G.B., Teoh A., Hobbs M., 2005, *ApJ*, 129, 1993
- MacFadyen A.I., Woosley S.E., 1999, *ApJ*, 524, 262
- Miyaji S., Nomoto K., Yokoi K., Sugimoto D., 1980, *PASJ*, 32, 303
- Muno M.P., Bauer F.E., Bandyopadhyay R.M., Wang Q.D., 2006a, *ApJSS*, 165, 173
- Muno M.P., Bower G.C., Burgasser A.J., Baganoff F.K., Morris M.R., Brandt W.N., 2006b, *ApJ*, 638, 183
- Nelemans G., Tout C.A., 2005, *MNRAS*, 356, 753
- Nice D.J., Sayer R.W., Taylor J.H., 1996, *ApJ*, 466, 87L
- O’Shaughnessy R., Kim C., Kalogera V., Belczynski K., 2005, *ApJ*, 672, 479
- O’Shaughnessy R., Kim C., Fragos T., Kalogera V., Belczynski K., 2005, *ApJ*, 633, 1076
- Paczynski B., 1967, *AcA*, 17, 287
- Paczynski B., 1976, in Eggleton P., Mitton S., Whelan J., eds, *Proc IAU Symp. 73, Structure and Evolution of Close Binary Systems*. Reidel, Dordrecht, p. 75
- Paczynski B., 1986, *ApJ*, 308, 43
- Paczynski B., 1990, *A&A*, 348, 485
- Petrovic J., Langer N., Yoon S.-C., Heger A., 2005, *A&A*, 435, 347
- Pfahl E., Podsiadlowski P., Rappaport S., 2005, *ApJ*, 628, 343
- Podsiadlowski Ph., Rappaport S., Han Z., 2003, *MNRAS*, 341, 385
- Portegies Zwart S.F., Verbunt F., 1996, *A&A*, 309, 179
- Portegies Zwart S.F., Yungelson L.R., 1998, *A&A*, 332, 173
- Ricker P.M., Taam R.E., 2008, *ApJ*, 672, 41
- Sadowski A., Belczynski K., Bulik T., Ivanova N., Rasio F.A., O’Shaughnessy R., 2008, *ApJ*, 676, 1162
- Savaglio S., Glazebrook K., & Le Borgne D., 2009, *ApJ*, 691, 101
- Stairs I.H., 2004, *Science*, 304, 547
- Stairs I.H., 2008, in Bassa C.G., Wang Z., Cumming A., Kaspi V.M., eds., *AIP Conf. Ser. Vol. 938, 40 Years of Pulsars – Millisecond Pulsars, Magnetars, and More*, American Inst. of Physics, New York, p. 424
- Steers J.A., 1970, *An Introduction to the Study of Map Projections*, University of London Press, London
- Taam R.E., Sandquist E.L., 2000, *ARA&A*, 38, 113
- Tauris T.M., Manchester R.N., 1998, *MNRAS*, 298, 625
- Tauris T.M., Dewi, J.D.M., 2001, *A&A*, 369, 170
- Taylor J.H., Fowler L.A., McCulloch P.M., 1979, *Nature*, 277, 437
- Taylor J.H., Manchester R.N., 1977, *ApJ*, 215, 885
- Tumlinson J, Prochaska J.X., Chen H-W., Dessauges-Zavadsky M., Bloom J.S., 2007, *ApJ*, 668, 667
- Tutukov A., Yungelson C., 1996, *MNRAS*, 280, 1035
- van den Heuvel E.P.J., 2007, in Antonelli A.L., et al. eds, *AIP Conf. Proc. Vol. 942, The Multicolored Landscape of Compact Objects and their Explosive Origins*. Am. Inst. Phys., New York, p. 598
- Vink J.S., de Koter A., Lamens H., 2001, *A&A*, 369, 574
- Voss R., Tauris T.M., 2003, *MNRAS*, 342, 1169
- Webbink R.F., 1984, *ApJ*, 277, 355
- Willems B., Henninger M., Levin T., Ivanova N., Kalogera V., McGhee K., Timmes F.X., Fryer C.L., 2005, *ApJ*, 625, 324
- Woosley S.E., 1993, *ApJ*, 405, 273
- Woosley S.E., Bloom J.S., 2006, *Annu. Rev. Astron. Astrophys.*, 44, 507
- Yoon S.-C., Langer N., Norman C., 2006, *A&A*, 460, 199
- Yusifov I., Kucuk I., 2004, *A&A*, 422, 545

This paper has been typeset from a \TeX / \LaTeX file prepared by the author.